Probing chirality structure in lepton-flavor-violating Higgs decay $h \to \tau\mu$ at the LHC

L. Zamakhsyari
Kanazawa University

M. Aoki, S. Kanemura, M. Takeuchi, and L. Z. *Phys. Rev. D* 107 (2023) 5

KEK, Phenomenology Meeting 2023
7.11.2023

Introduction and background

Motivation

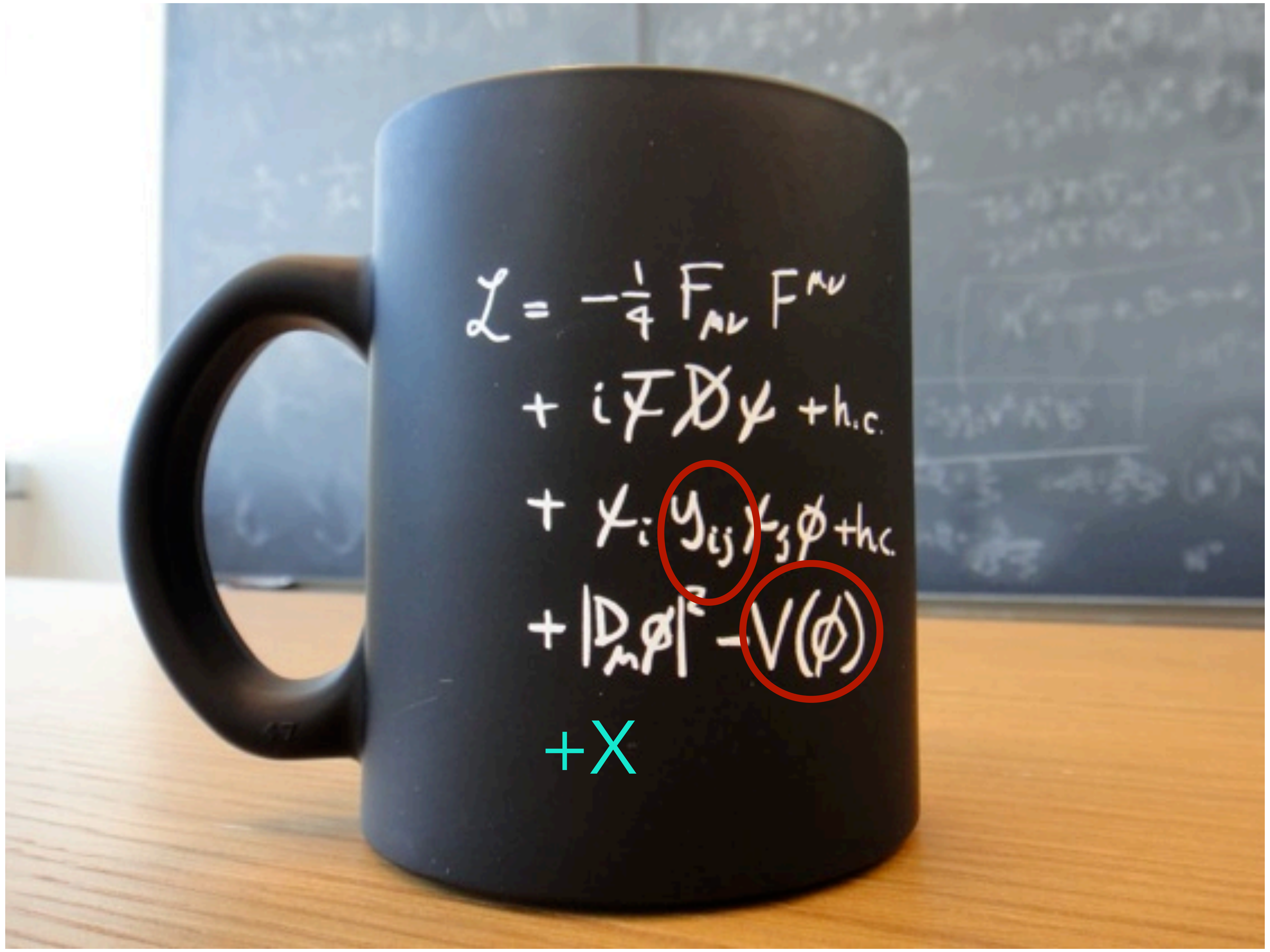

After $m_h = 125$ GeV in 2012

Standard model (SM) is not finished yet…

1. Flavor structure.
2. Higgs sector.
3. BSM phenomena : neutrino mass, DM, Baryon asymmetry.
4. Gravity unification

Focus : flavor structure especially the lepton-flavor violation (LFV)

$(h \to l_i l_j,\ l_i \to l_j \gamma, \text{etc.})$

testable at previous, current and future experiments.

(Charged) LFV interaction

In SM : Higgs only couple to same flavour leptons.

$$-\mathscr{L}_Y^{\rm SM} \supset \overline{l_L}\frac{Y_1}{\sqrt{2}}l_R h + h.c., \quad m_l = \mathrm{diag}(m_e, m_\mu, m_\tau) = \frac{v}{\sqrt{2}}V_L^\dagger Y_1 V_R$$

In BSM : an extra Yukawa matrix -> can not be diagonalized simultaneously -> Source of LFV.

$$-\mathscr{L}_Y \supset \overline{l_L}\left(\frac{Y_1}{\sqrt{2}} + \frac{Y_2}{\sqrt{2}}\right)l_R h + h.c.,$$

Example in 2HDM (type III):

$$-\mathscr{L}_Y^{\rm 2HDM} \supset \overline{l_L}\underbrace{\left(\frac{m_l}{v}\sin(\beta-\alpha) + \frac{\rho^l}{\sqrt{2}}\cos(\beta-\alpha)\right)}_{y} l_R h + h.c.$$

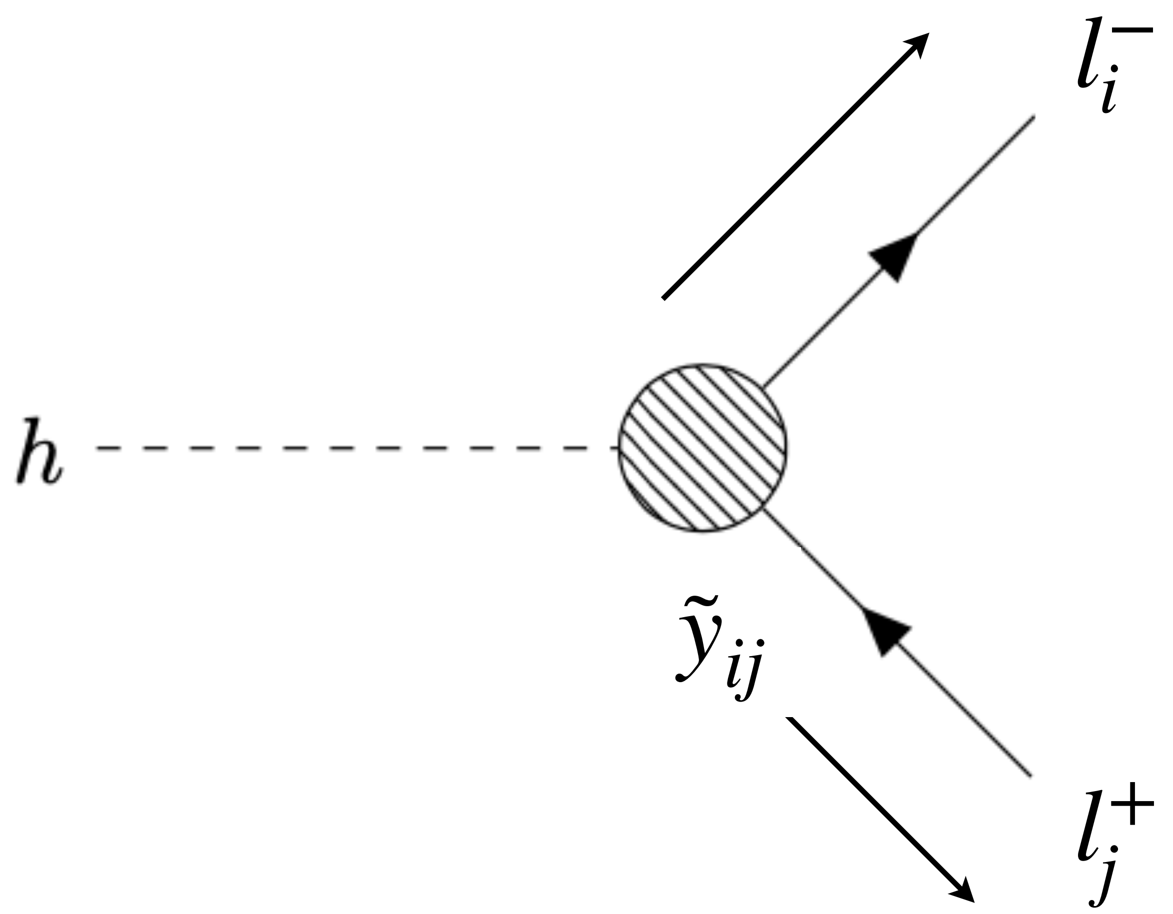

$$y = \begin{pmatrix} y_{ee} & y_{e\mu} & y_{e\tau} \\ y_{\mu e} & y_{\mu\mu} & y_{\mu\tau} \\ y_{\tau e} & y_{\tau\mu} & y_{\tau\tau} \end{pmatrix}$$

$$-\mathscr{L}_{\rm Y} \supset \bar{l}_i(y_{ij}P_R + y_{ji}^* P_L)hl_j = \bar{l}_i\tilde{y}_{ij}hl_j$$

LFV Higgs decay (hLFV)

- hLFV only processes $h \to l_i l_j$ $(h \to l_i^+ l_j^- + h \to l_i^- l_j^+)$.
  1. Extensive experimental records on $h \to l_i l_j$ at the LHC.
  2. Upgrade on future HL-LHC up to L=3000 fb^{-1}.

     [CERN Yellow Rep. (2015) 5]: more data available to be analyzed.
- Which $h \to l_i l_j$?
  1. $\bar{y}_{ij}$ on $h \to l_i l_j$ is strongest among all LFV, except $\mu - e$.

     $\bar{y}_{\mu e}$: $\sim 10^{-4}$ $(h \to \mu e)$ << $\sim 10^{-6}$ $(\mu \to e\gamma)$. $h \to \mu e$ is not considered.
  2. $h \to \tau e$ has more backgrounds than $h \to \tau\mu$.
- $h \to \tau\mu$ only.

Process	BR (ATLAS)		BR(CMS)	
$h \to \mu e$	6.2×10^{-5}	[1]	4.4×10^{-5}	[2]
$h \to \tau e$	2.0×10^{-3}	[3]	2.2×10^{-3}	[4]
$h \to \tau\mu$	1.8×10^{-3}	[3]	1.5×10^{-3}	[4]

[1] ATLAS, Phys. Lett. B 801 (2020)

[2] CMS, Phys.Rev.D 108 (2023) 7

[3] ATLAS, JHEP 07, 166 (2023)

[4] CMS, Phys.Rev.D 104 (2021) 3

$$BR \sim \bar{y}_{ij}^2, \quad \bar{y}_{ij} \equiv \sqrt{|y_{ij}|^2 + |y_{ji}|^2}$$

Chirality structure

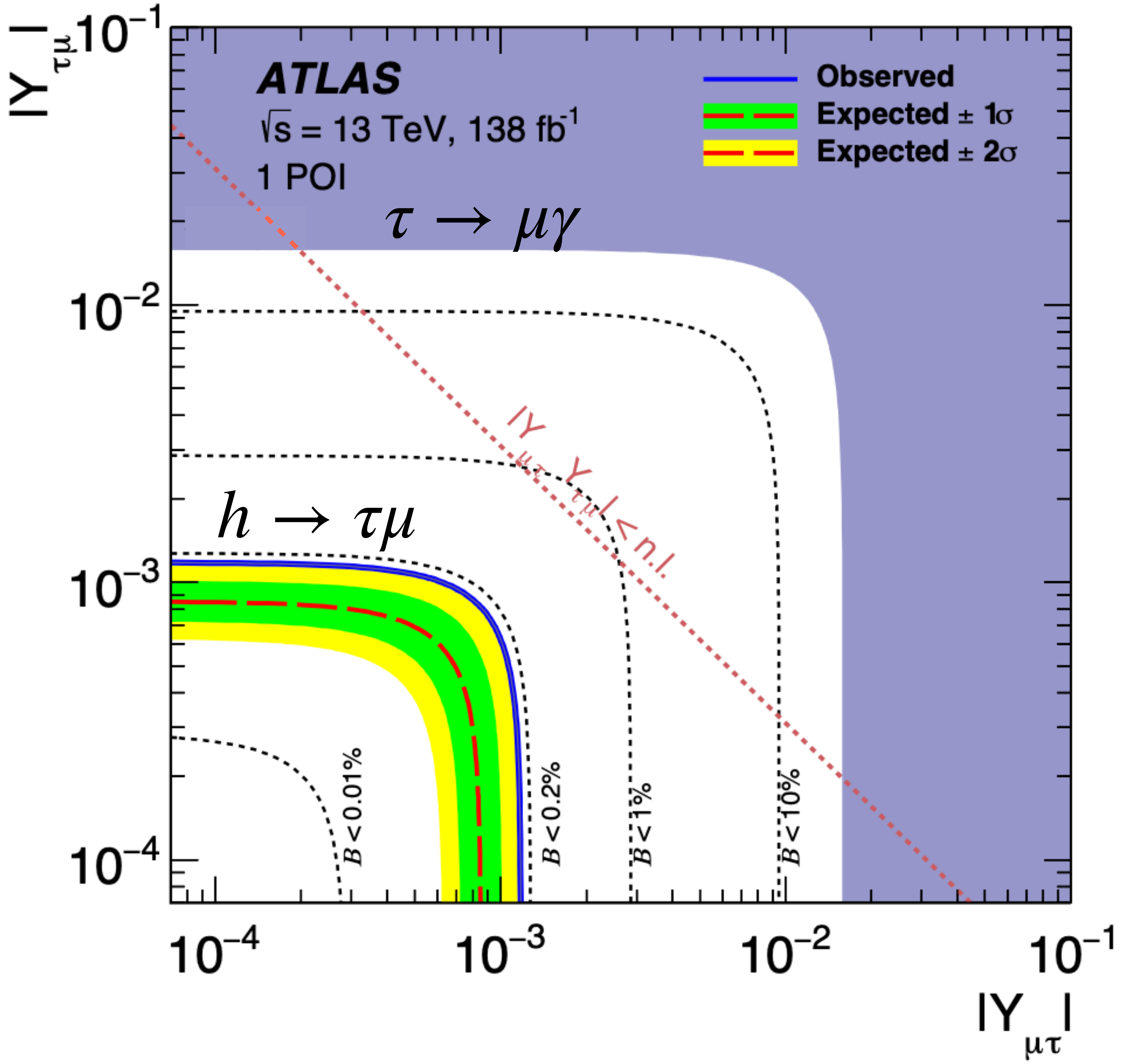

ATLAS, JHEP 07, 166 (2023)

$$\bar{y}_{\tau\mu} = \sqrt{|y_{\tau\mu}|^2 + |y_{\mu\tau}|^2} < 1.2 \times 10^{-3}\ (h \to \tau\mu)$$

- Unpolarized. no chirality preference : $h \to \tau\mu$.

  Experiment/simulation to derive upper limit (UL)

  $BR(h \to \tau\mu) \propto |y_{\tau\mu}|^2 + |y_{\mu\tau}|^2 <$ some number.

  -> circle area on the $|y_{\mu\tau}| - |y_{\tau\mu}|$ plane.

- Polarized case : $h \to \tau_L\mu_R, h \to \tau_R\mu_L$.

  UL: $BR(h \to \tau_L\mu_R) \propto |y_{\tau\mu}|^2$ < number 1

  $BR(h \to \tau_R\mu_L) \propto |y_{\mu\tau}|^2$ < number 2

- The UL contour will be contribution from both that will modify the shape of the contour.

- Theoretically some BSM models induce a natural chiral structure on hLFV.

  [C. W. Chiang, et. al., JHEP 11 (2015) 057] (axion-variant)

  2HDM + singlet scalar σ with PQ charge $(0, -1, +1)$ for (Φ_1, Φ_2, σ).

  τ_R PQ charge = -1.

$$\mathscr{L}_Y \supset \sum_{i,a} \bar{l}_{Li}(Y_1)_{ia}\Phi_1 l_{Ra} + \bar{l}_{Li}(Y_2)_{i3}\Phi_2\tau_R + h.c., \quad i = 1,2,3, \quad a = 1,2$$

$$\mathscr{L}_Y \supset -\sum_{l=e,\mu,\tau} \xi_l \frac{m_l}{v}\bar{l}l - a \sum_{l,l'=e,\mu,\tau} (H_l)_{ll'}\frac{m_l}{v} h\bar{l}_L l'_R + h.c.$$

H_l is the Hermitian, non diagonal flavor matrix.

$h \to \tau\mu$ -> $h \to \tau_L\mu_R \quad : y = (H_l)_{\tau\mu} m_\tau / v,$ $\qquad h \to \tau_R\mu_L \quad : y = (H_l)^*_{\mu\tau} m_\mu / v$

$h \to \tau\mu$ -> $h \to \tau_L\mu_R$

Objectives

- If $h \to \tau\mu$ is polarized, what is the effects on the coupling contour in $|y_{\mu\tau}| - |y_{\tau\mu}|$ plane.
- Is the chirality structure distinguishable?

Simulations and Results

Chirality structure : tau polarization

- In principle the τ polarization (τ_R, τ_L) information is carried by its decay products.
- $pp \to h \to \tau\mu \to \tau_h \nu_\tau \mu$, τ_h is visible hadronic tau decay products : π, ρ, a_1 (made up more than 50% of tau BR).
- Distribution of energy fraction $x_i = E_i / E_\tau$, $i = \pi, \rho, a_1$.
- Simulation is done in Madgraph by fixing $(y_{\mu\tau}, y_{\tau\mu}) = (1,0); (0,1)$ for τ_R, τ_L respectively.
- At parton level and reconstructed level.

Tau polarization : Parton level

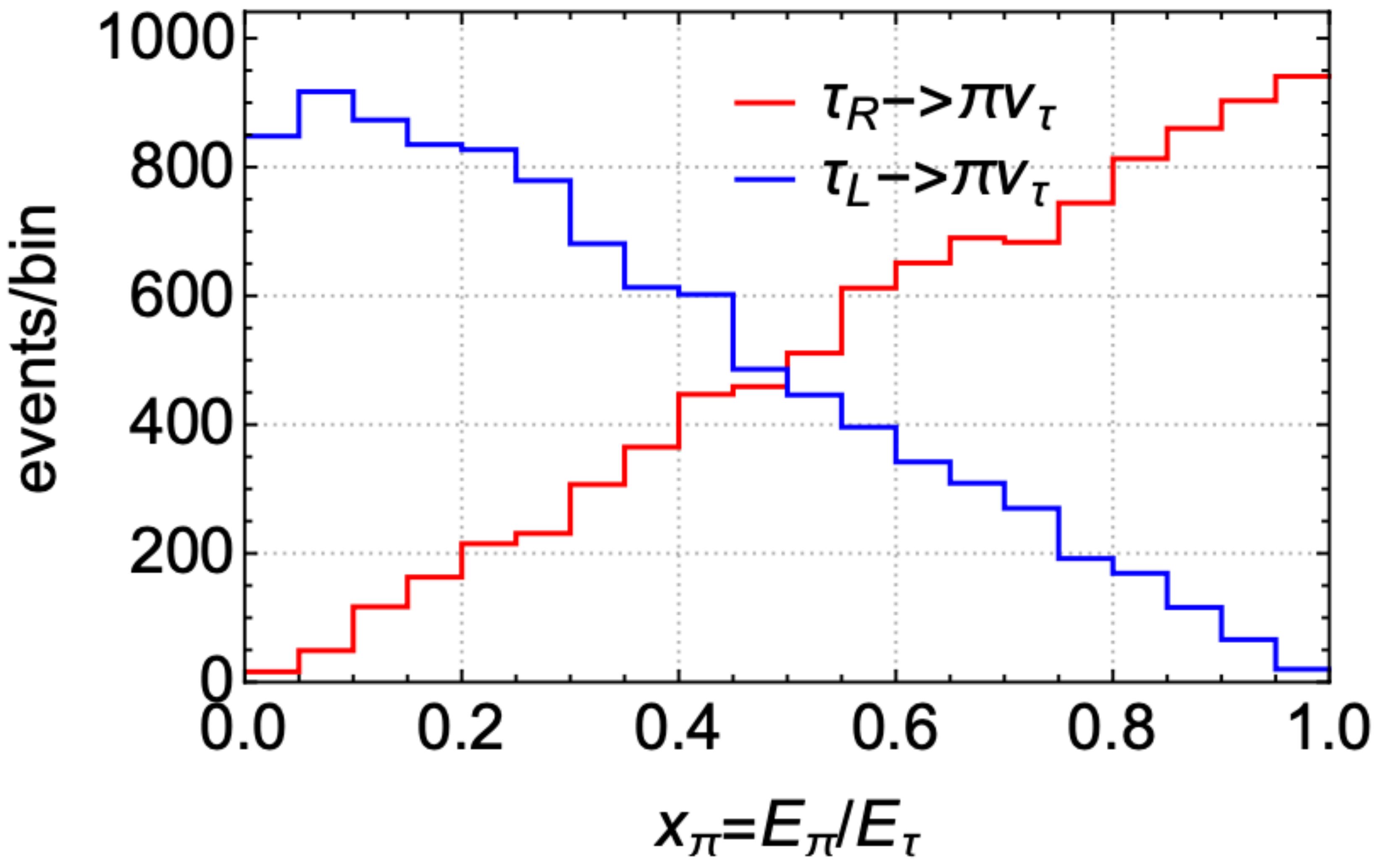

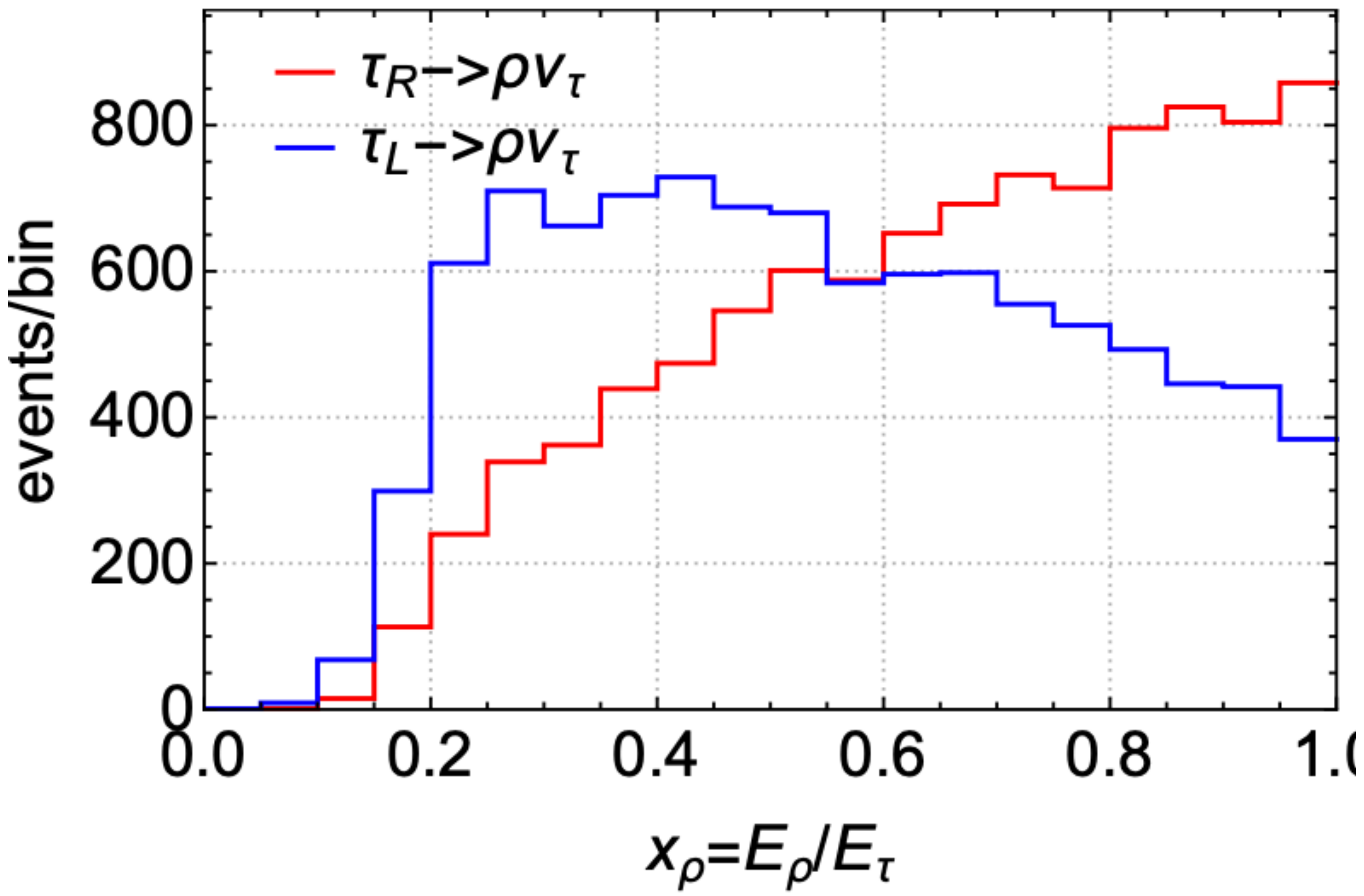

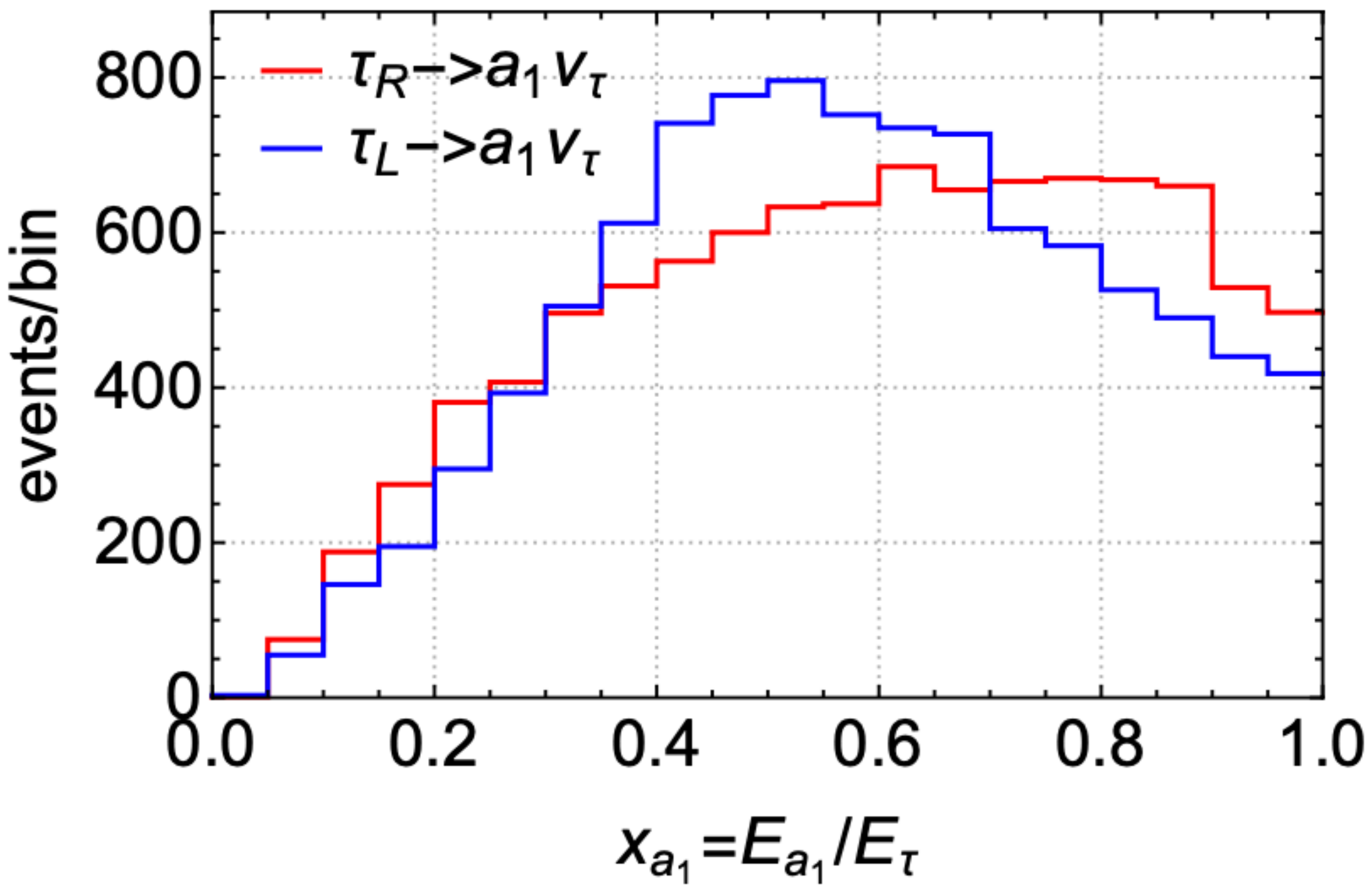

- Clear separation between τ_R, τ_L : hard on τ_R and soft on τ_L. Very clear in x_π. The distributions agree with [B. K. Bullock, et.al, Nucl. Phys. B 395, 499 (1993), K. Hagiwara, et.al., Phys. Lett. B 235, 198 (1990)]
- On ρ, a_1 the τ_R, τ_L structure are sensitive on high x but not too sensitive in low x .

Tau polarization : Reconstructed level

- Reconstructed level done by simulating the detector using Delphes.
- Significant reduction at the low x_i due to jet energy threshold. Original shapes still preserved.
- The polarization affects the acceptance of number of events.

Signal and background simulation at the LHC

$\sqrt{s} = 13$ TeV, $L = 36.1\mathrm{fb}^{-1}$.

- Signal : $pp \to h$ (ggf), $\mathrm{h} \to \tau\mu \to \tau_{\mathrm{h}}\nu_\tau\mu$.
- Chirality structure : $(y_{\mu\tau}, y_{\tau\mu})$= (0,1) ,(1,0) for $h \to \tau_L\mu_R, h \to \tau_R\mu_L$.
- Background : $pp \to Z, Z \to \tau_h\tau_\mu$. τ_μ are taus decay to muons.

	Selection cuts
Baseline	exactly 1μ and 1τ jet (opposite sign)
	$p_{T,\mu} > 27.3$ GeV, $p_{T,\tau_{\rm vis}} > 25$ GeV
	$\lvert\Delta\eta(\mu, \tau_{\rm vis})\rvert < 2.0$
	$\sum_{i=l,\tau_{\rm vis}} \cos\Delta\phi(i, \not{E}_T) > -0.35$

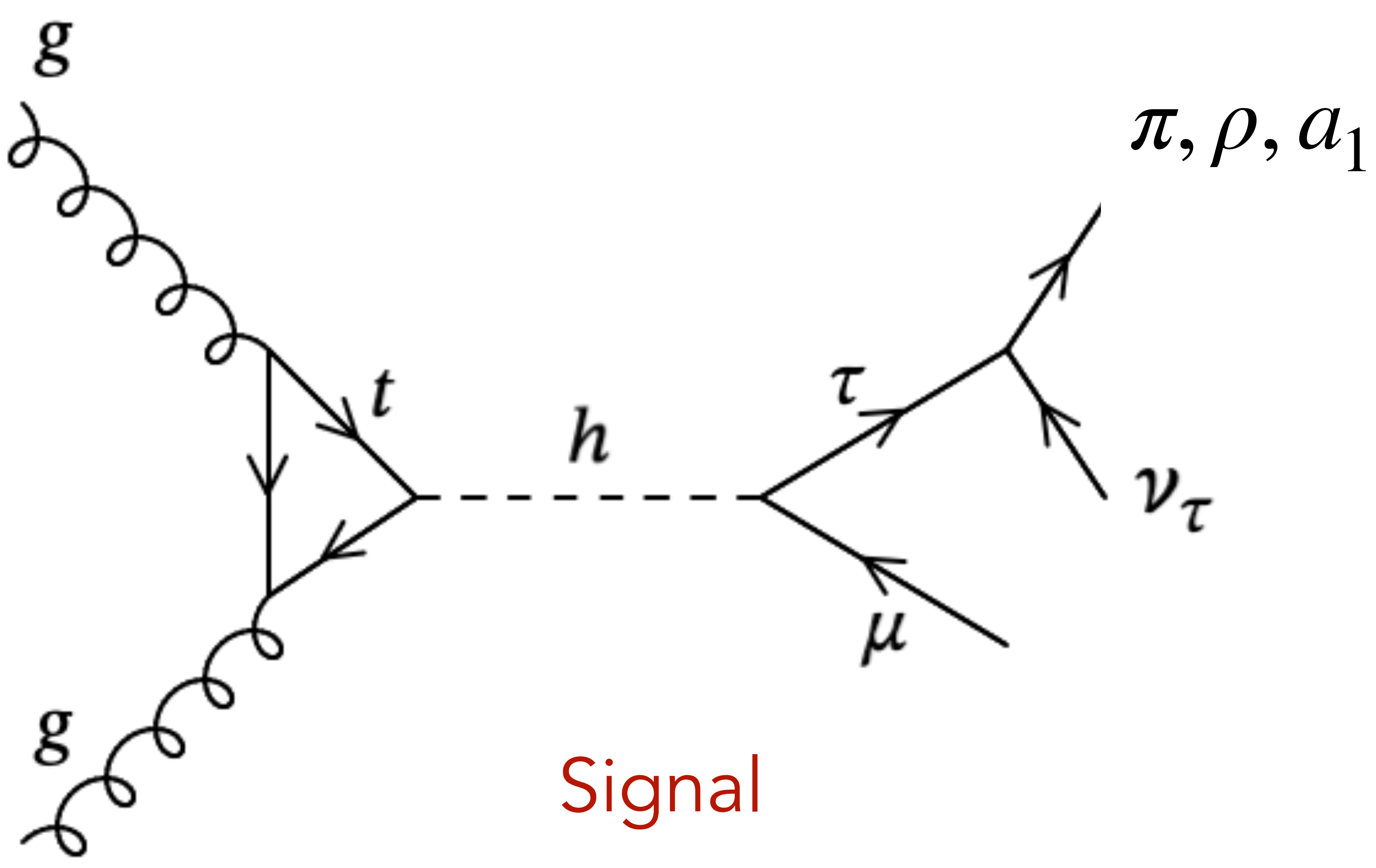

Signal

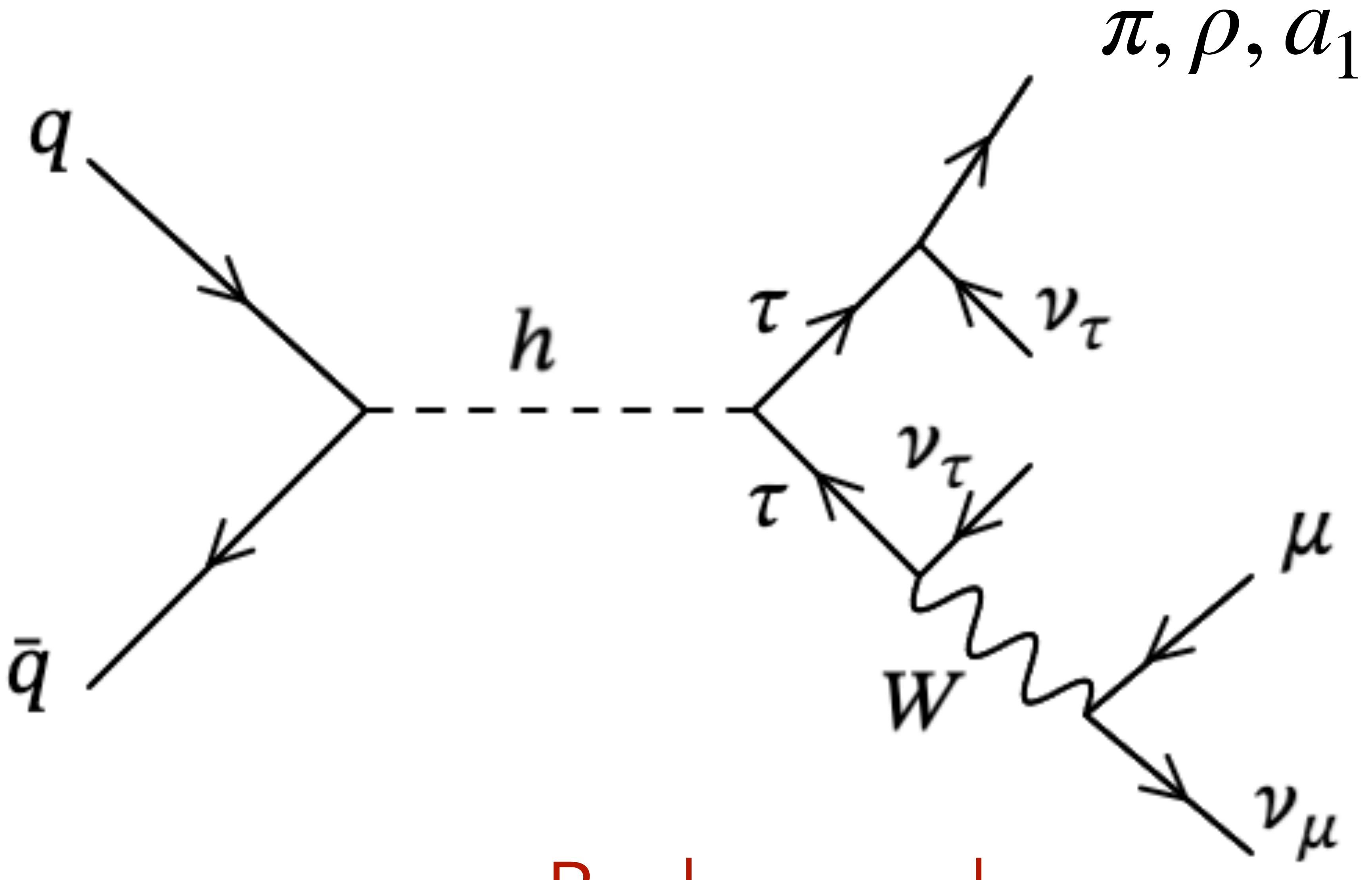

Background

Collinear mass analysis

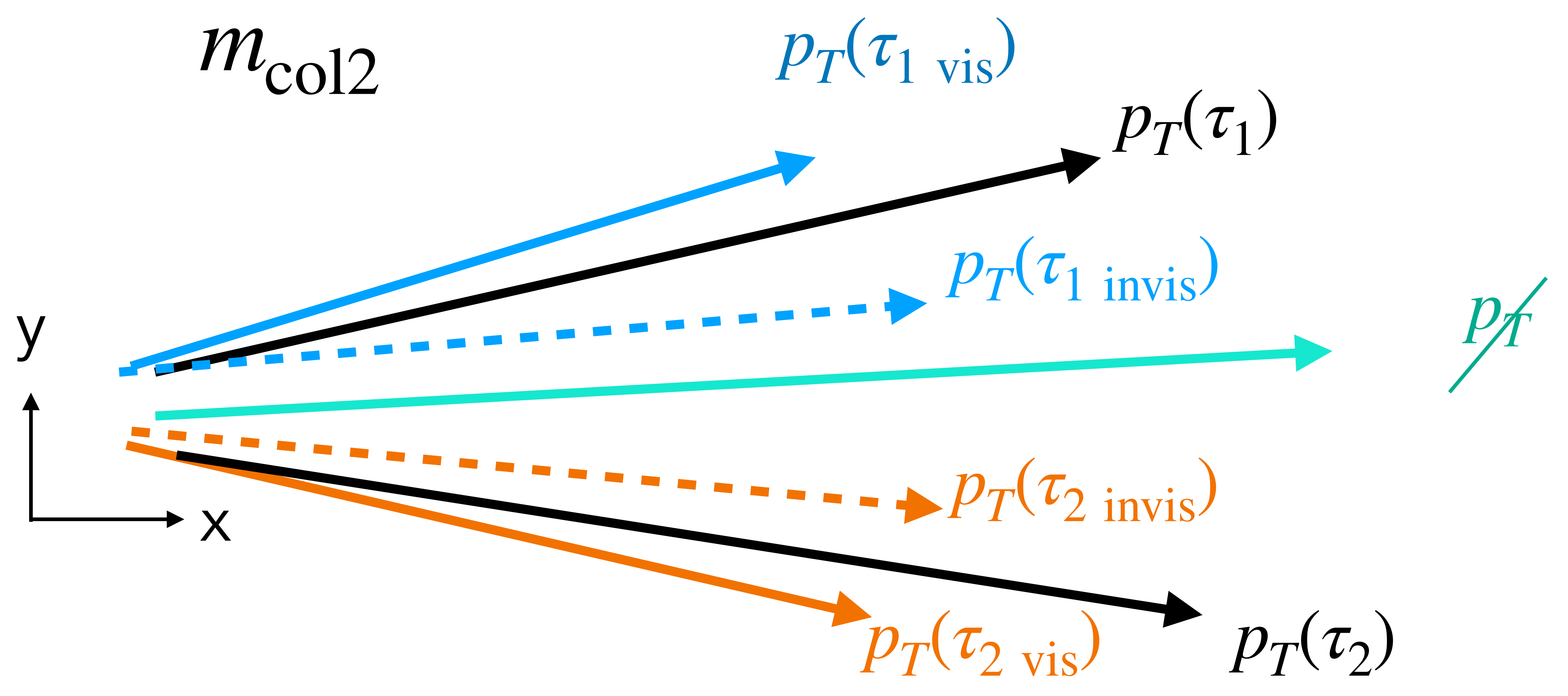

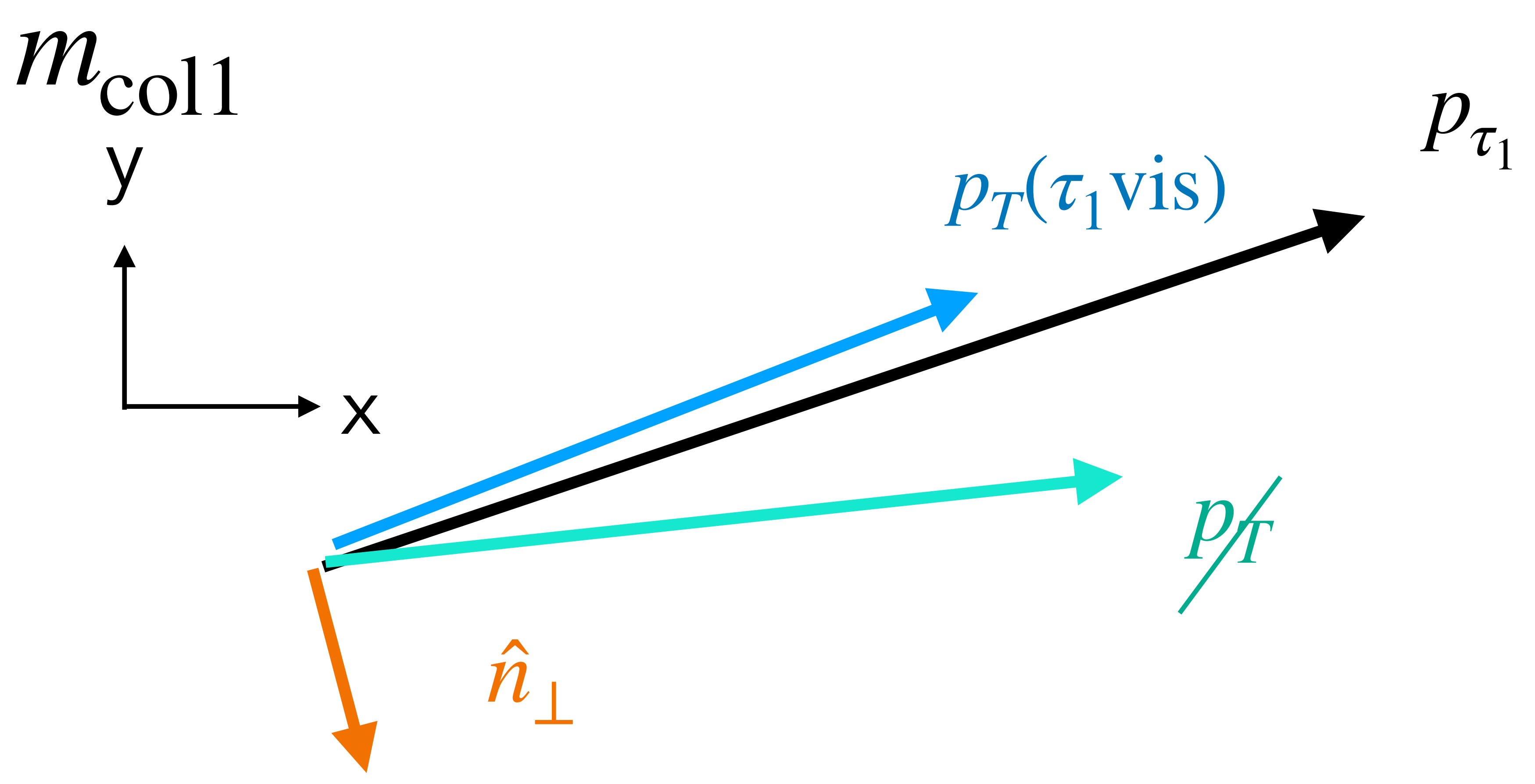

- Based on $m_{\tau\tau}$ reconstruction.
- $\vec{\not{p}}_T = \vec{p}_T(\tau_{1\ \text{invis}}) + \vec{p}_T(\tau_{2\ \text{invis}}) \equiv c_1\vec{p}_T(\tau_{1\ \text{vis}}) + c_2\vec{p}_T(\tau_{2\ \text{vis}}), \quad c_i > 0$
  [M. Schlaffer, et. al.,Eur.Phys.J.C 74 (2014) 10]
- Solving $c_{1,2}$: $m^2_{\text{col2}} = (p_{\tau_{1\text{vis}}} + p_{\nu_{1,}} + p_{\tau_{2\text{vis}}} + p_{\nu_2})^2$
- For $m_{\tau\mu}$, $\mu \equiv \tau_{2\ \text{vis}}$. [R. Harnik, et.al., *JHEP* 03 (2013) 026]

- Construction with 1 τ_{vis}.
- Although $\vec{p}(\tau_{1\ \text{invis}}) \equiv c_1\vec{p}(\tau_{1\ \text{vis}})$, $\vec{\not{p}}_T$ is not completely parallel with $\vec{p}_{T,\tau_{1\ \text{vis}}}$:
  $\vec{\not{p}}_T = c_1\vec{p}_{T,\tau_{1\ \text{vis}}} + c_\perp\hat{n}_{T,\perp}$,
- Solving for c_1: $m^2_{\text{col1}} = (p_{\tau_{1\text{vis}}} + p_{\nu_1} + p_\mu)^2$.

The distribution of m_{col2} and m_{col1}

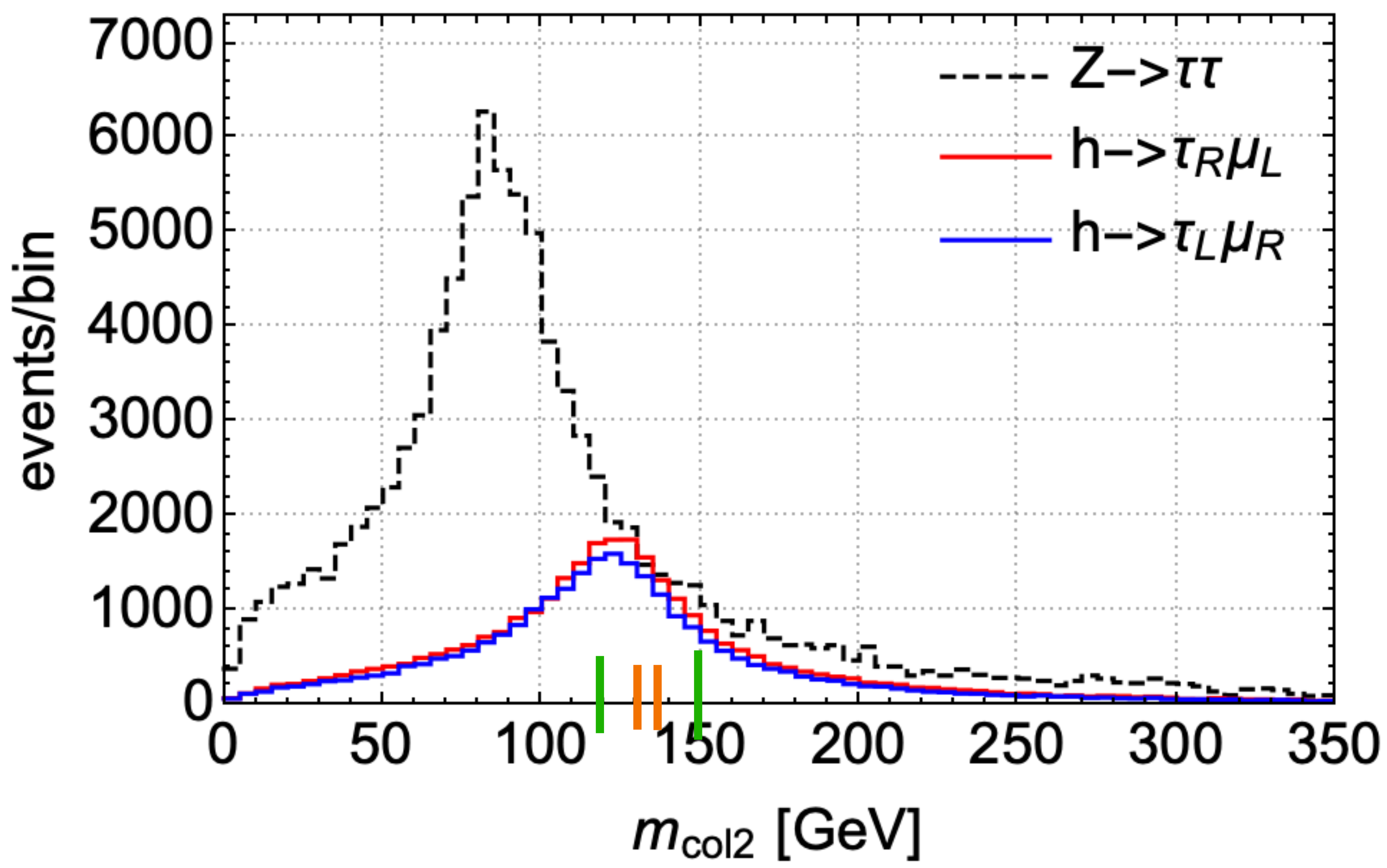

,

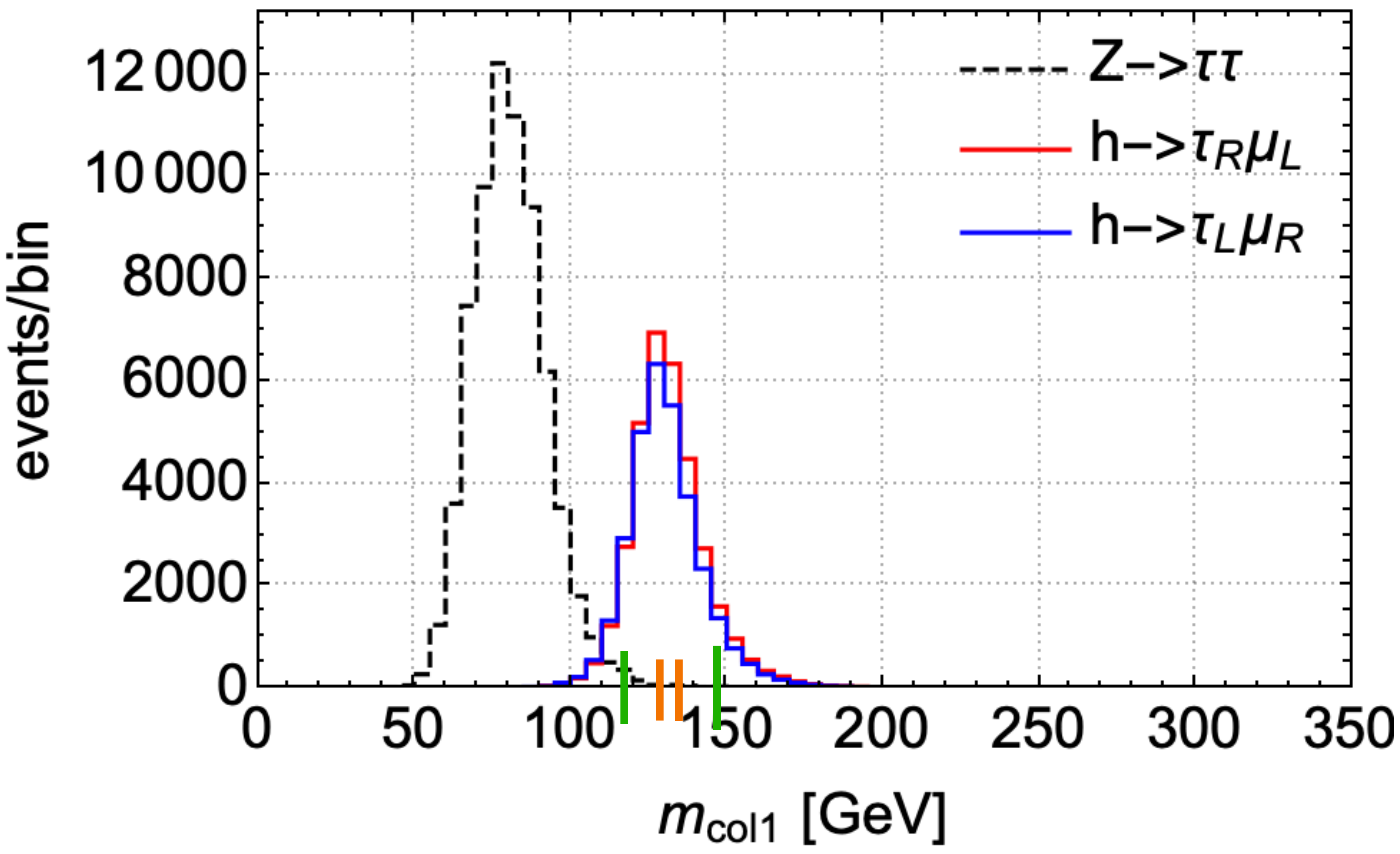

- m_{col1} has a sharper peak and clear separation between S and B than m_{col2}.
- Better signal region using $|m_{\text{coll}i} - m_h| < \Delta m$, with Δm = **25** and **5** GeV.

Cut flows for signal and background

		Signal (S) $h \to \tau\mu_{(BR=1\ \%)}$ τ_R	Signal (S) $h \to \tau\mu_{(BR=1\ \%)}$ τ_L	Background (B) $Z \to \tau_h \tau_\mu$
	σ at 13 TeV LHC	355 fb		258 pb
	for $\mathcal{L} = 36.1\text{fb}^{-1}$	12795		9.31×10^6
	baseline cuts	1979	1742	130147
m_{coll2}	$x_1 > 0$ and $x_2 > 0$	1672	1480	102536
	$\lvert m_{\text{coll2}} - m_h \rvert < 25$ GeV	717	643	21473
m_{coll1}	$c_1 > 0$	1765	1608	68602
	$\lvert m_{\text{coll1}} - m_h \rvert < 25$ GeV	1626	1493	4023

$x_i = 1/(c_i + 1)$

The number of events are normalized to ATLAS 36.1 fb^{-1}.
[Phys. Lett. B 800, 135069 (2020)]

S/B

- No systematic error : better S/B.

m_{col2}

B ↓ : 0.23%
S ↓ : 5.5%
S/B=0.03

m_{col1}

B ↓ : 0.04%
S ↓ : 12.5%
S/B=0.39

- S/B is better for m_{coll}. $\Delta m = 5$ GeV, S/B=2.8.

Signal
(S)

	$h \to \tau\mu_{(BR=1\ \%)}$		
	τ_R	τ_0	τ_L
σ at 13 TeV LHC	355 fb		
for $\mathcal{L} = 36.1\text{fb}^{-1}$	12795		
baseline cuts	1979	1861	1742
$m_{\rm coll2}$: $x_1 > 0$ and $x_2 > 0$	1672	1576	1480
$m_{\rm coll2}$: $\lvert m_{\rm coll2} - m_h \rvert < 25$ GeV	717	680	643
$m_{\rm coll1}$: $c_1 > 0$	1765	1682	1608
$m_{\rm coll1}$: $\lvert m_{\rm coll1} - m_h \rvert < 25$ GeV	1626	1560	1493

$x_i = 1/(c_i + 1)$

The number of events are normalized to ATLAS 36.1 fb^{-1}.
[Phys. Lett. B 800, 135069 (2020)]

Chirality structure

- Asymmetry number of signals, $S(\tau_R) > S(\tau_L)$.
- $\pm 6\,\%$ difference with τ_0 for $m_{\rm col1}$ and $m_{\rm col2}$.
- $\Delta m = 5$ GeV, polarization sensitivity for $m_{\rm col1}$ reduced to 3.3% while for $m_{\rm col2}$ stays at 6%.

Sensitivity to the chirality structure

$\Delta m = 25$ GeV

	$S^{95\%}$	$\mathrm{BR}^{95\%}$ (%)			$\bar{y}_{\tau\mu}^{95\%}$		
		τ_R	τ_0	τ_L	τ_R	τ_0	τ_L
m_{col2}	342	0.48	0.50	0.53	0.0020	0.00205	0.0021
m_{col1}	148	0.091	0.095	0.099	0.00087	0.00089	0.00090

1. $S^{95\%} = 1.65\sqrt{B}$ is the frequentist one-sided 95% CL signal upper bound.
2. $BR^{95\%} = (S^{95\%}/S)\mathrm{BR}(h \to \tau\mu)$, with $\mathrm{BR}(\mathrm{h} \to \tau\mu) = 1\,\%$.
3. $\mathrm{BR} = 0.12\% \times \dfrac{(|y_{\mu\tau}|^2 + |y_{\tau\mu}|^2)}{10^{-6}}$ for τ_L, τ_R.
4. Any distribution $f(x; y_{\mu\tau}, y_{\tau\mu}) = |y_{\mu\tau}| f_R(x) + |y_{\tau\mu}| f_L(x)$

   $(y_{\mu\tau}, y_{\tau\mu})$:

   $\tau_L \sim (0,1), \quad \tau_R \sim (1,0), \quad \tau_0 \sim (1/2,1/2)$

Modification on $|y_{\mu\tau}| - |y_{\tau\mu}|$ contour

$\Delta m = 25$ GeV

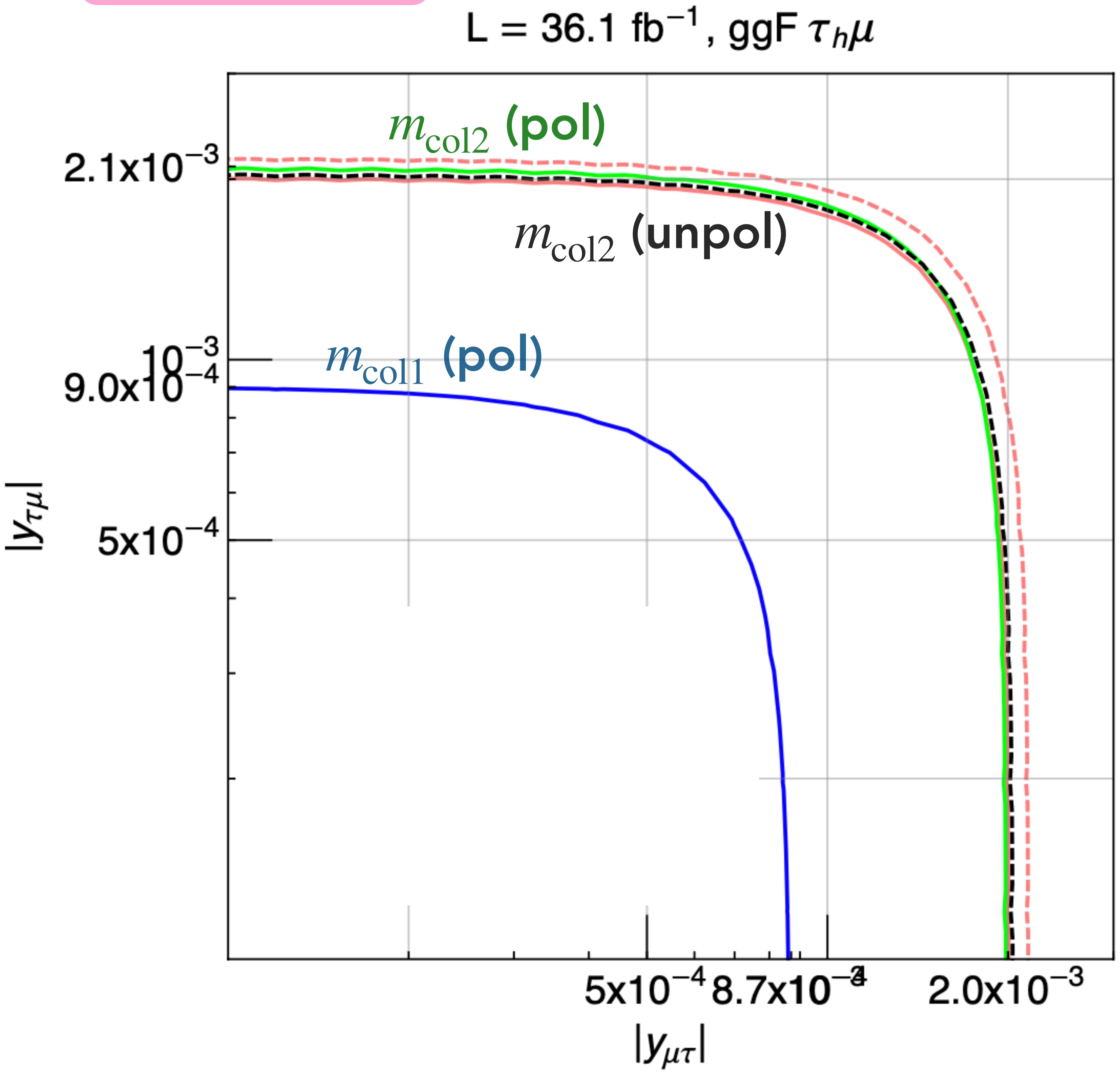

- Modification on the sensitivity contour from circle (unpolarized) to ellipse (polarized)
- $m_{\rm col2}$ **polarized** -> **unpolarized** modify the contour up to $\pm 2-3\,\%$ on $y_{\mu\tau} - y_{\tau\mu}$ (BR up to $\pm 4 - 6\,\%$).
- The sensitivity is improved 5 times from $m_{\rm col2}$ to $m_{\rm col1}$.

$\Delta m = 25$ GeV

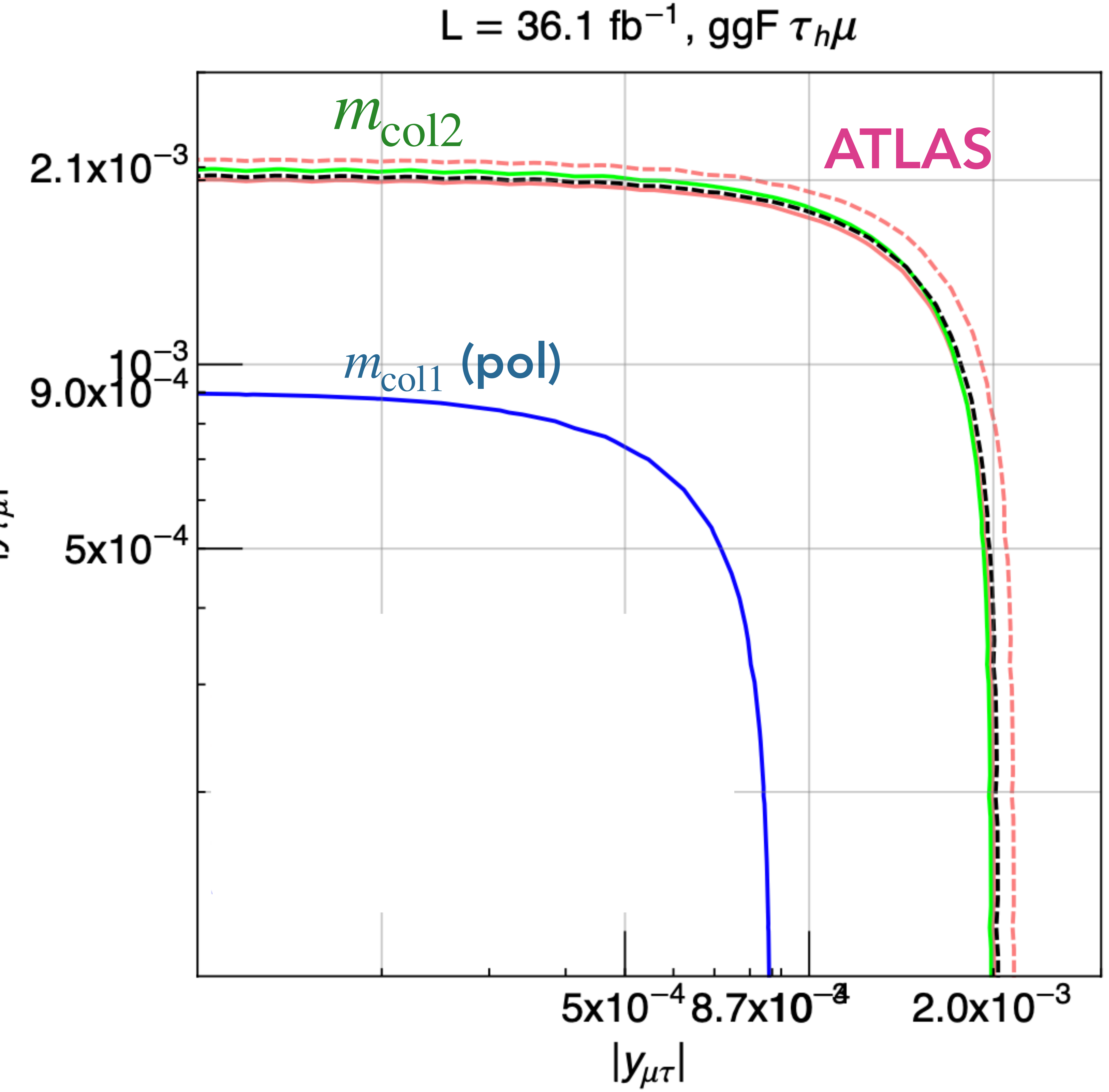

Comparison to ATLAS 36.1 $\rm fb^{-1}$expected result

- $m_{\rm col2}$ appeared to be close to the ATLAS expected result (dashed-pink). If systematic error analysis is included, the sensitivity by $m_{\rm col2}$ analysis will be worse. However, $m_{\rm col1}$ has a better sensitivity should persist.

Expected result ATLAS
BR($h \to \tau\mu) = 0.57\,\%$ (non-VBF)
$\bar{y}_{\tau\mu} = 0.0022$

Sensitivity for the chirality structure

- Probing the chirality structure given a finite number of signals.
- Scenarios BR($h \to \tau\mu$)=0.12% or $\bar{y}_{\tau\mu} = 10^{-3}$:

$$(\hat{y}_{\mu\tau}, \hat{y}_{\tau\mu}) = \begin{cases} (10^{-3},0), & \tau_R \\ (0,10^{-3}), & \tau_L \\ (7.1 \times 10^{-4},7.1 \times 10^{-4}), & \text{unpolarized} \end{cases}$$

- x_1 distribution of m_{coll1}. Two signal regions (SR) : SR1 ($x_1 < 0.6$) and SR2 ($x_1 \geq 0.6$).

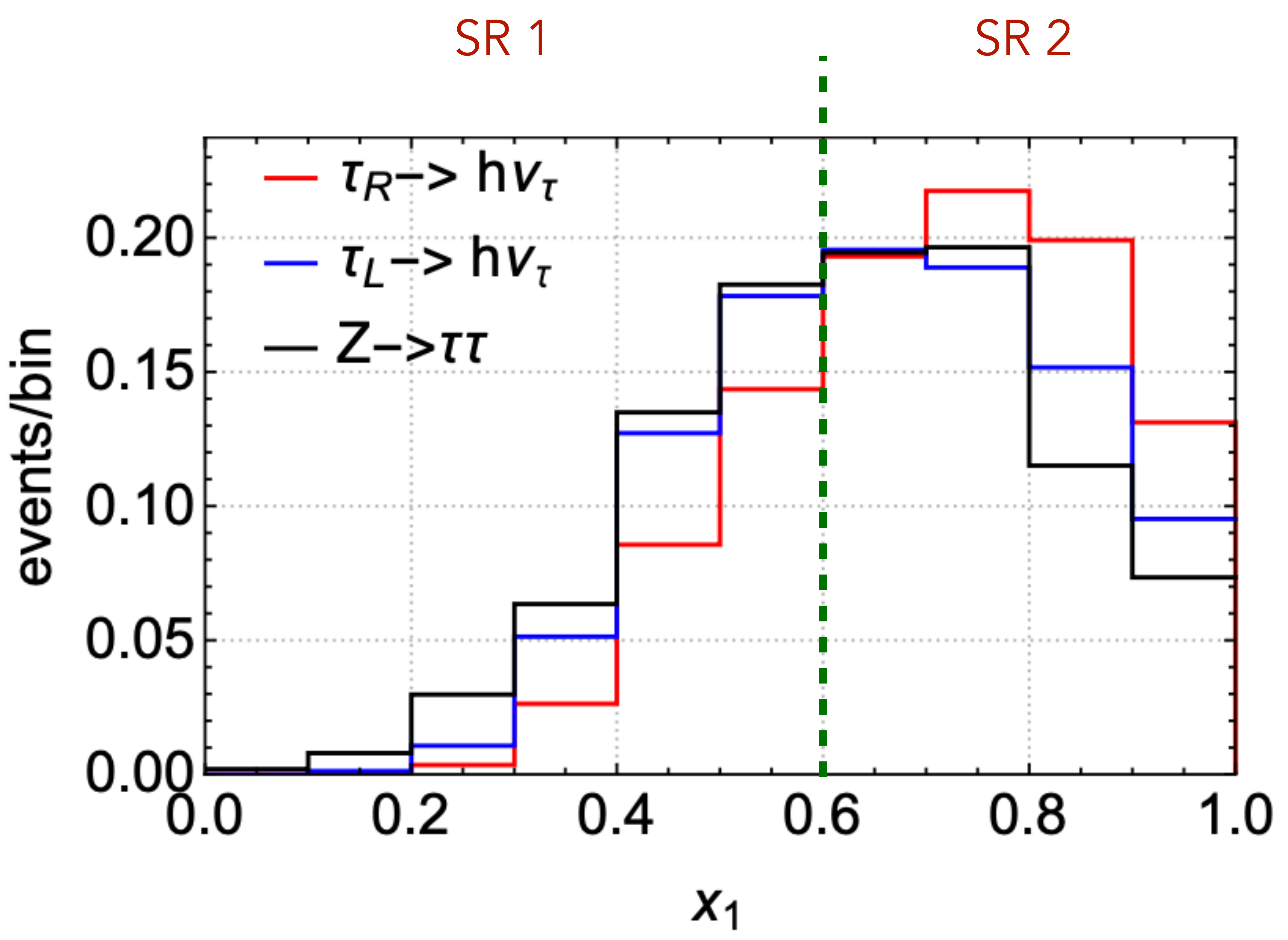

m_{coll1}, $\Delta m = 25$ GeV, L=36.1 fb^{-1}

$\Delta m_{\text{coll}}^{\text{th}}$	SR	$N_{i,BR=0.12\%}$			N_i/N		$N_{i,\text{obs}}$ for each scenario		
		τ_R	τ_L	$Z\to\tau\tau$	τ_R	τ_L	τ_R	τ_0	τ_L
25 GeV	SR_1	50.6	66.1	3384	0.26	0.37	3436	3443	3451
	SR_2	144.5	113.1	2331	0.74	0.63	4807	4791	4776
	total	195.1	179.2	8046	1	1	8243	8234	8227

$$N_{i,\text{obs}} = S_i + B_i$$

- Expected contour region deviates from the observed events in each scenario : χ^2 two dimensional parameter fit.

$$\chi^2 = \left(\frac{N_{1,\text{exp}} - N_{1,\text{obs}}}{\sqrt{N_{1,\text{exp}}}}\right)^2 + \left(\frac{N_{2,\text{exp}} - N_{2,\text{obs}}}{\sqrt{N_{2,\text{exp}}}}\right)^2 \quad \text{->} \quad \chi^2 = \left(\frac{r\Delta N_R + l\Delta N_L}{\sqrt{N_{1,\text{obs}}}}\right)^2 + \left(\frac{(1-r)\Delta N_R + (1-l)\Delta N_L}{\sqrt{N_{2,\text{obs}}}}\right)^2$$

$\Delta N_R = N_R \left(\frac{L}{36.1\ \text{fb}^{-1}}\right)\frac{(y_{\mu\tau} - \hat{y}_{\mu\tau})^2}{10^{-6}}$, $\Delta N_L = N_L \left(\frac{L}{36.1\ \text{fb}^{-1}}\right)\frac{(y_{\tau\mu} - \hat{y}_{\tau\mu})^2}{10^{-6}}$ are the deviations from the value N_R and N_L. $r, l = (N_1/N)_{R,L}$.

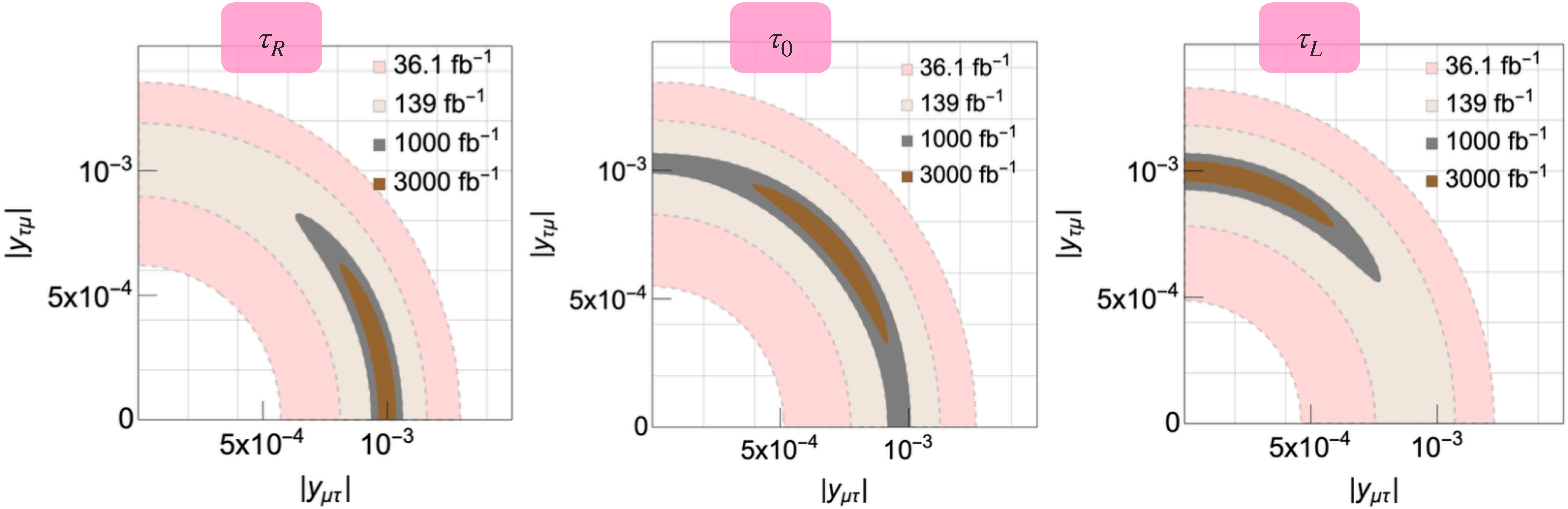

$\chi^2 < 2.3\ (1\sigma)$

- τ_R, τ_L can be distinguished at $2.3\sigma(4.4\sigma)$ for 1000(3000) fb^{-1} and τ_0 can be distinguished at 1.9 σ at 3000 fb^{-1}.

- $\Delta m = 5$ GeV. τ_R, $\tau_0(\tau_L)$ can already be distinguished at $2.1\sigma(4.8\sigma)$ for 139 fb^{-1}.

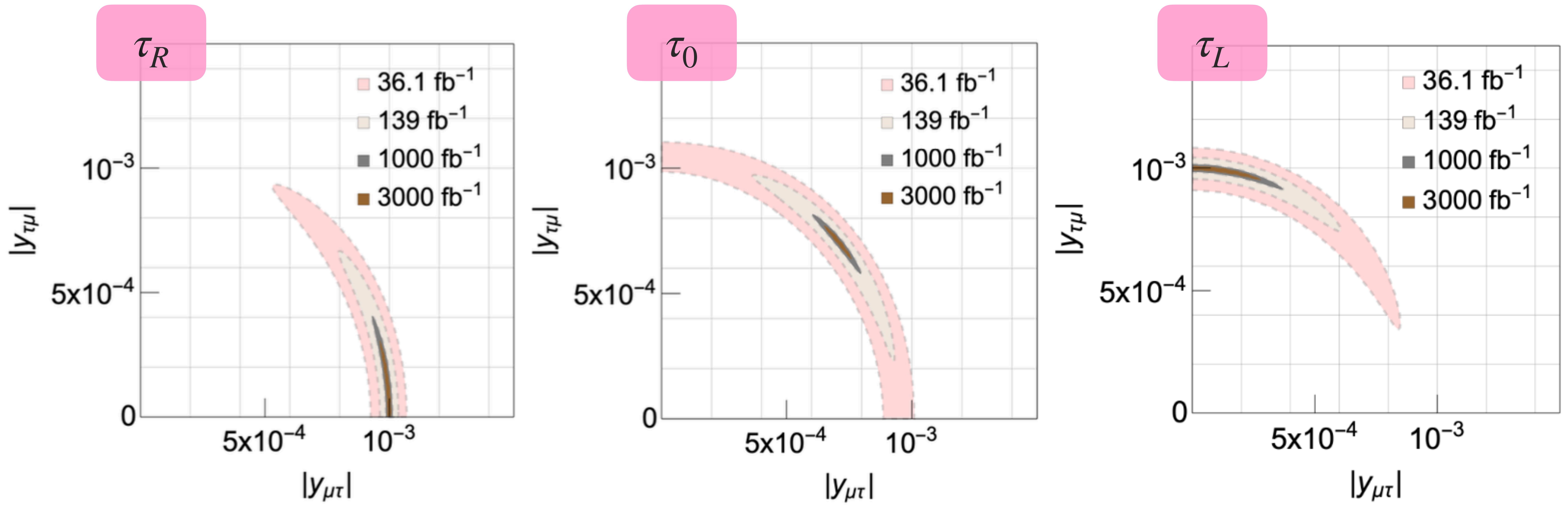

Conclusion

1. Polarization affects the acceptance of number of events.
2. The collinear mass $m_{\rm col1}$ gives a better S/B ratio for signal-background analysis on hLFV $h \to \tau\mu$ than $m_{\rm col2}$.
3. The sensitivity on the $\bar{y}_{\tau\mu}$ is modified up to $\pm 2 - 3\,\%$ due to the polarization for $\Delta m = 25$ GeV.
4. Chirality structure can be probed at the near future HL-LHC :
   a. For Δm =25 GeV, τ_R, $\tau_L$can be distinguished at least at 1000 fb^{-1} with confidence 2.3σ and τ_0 at 3000 fb^{-1} with1.9σ.
   b. For $\Delta m = 5$ GeV, the chirality structure will become sensitive at 139 fb^{-1}. Assuming τ_R, $\tau_0(\tau_L)$ can be distinguished at 2.1$\sigma(4.8\sigma)$.

Thank You
ありがとうございます

Theory : Tau chirality

- The tau chirality : spin polarization (helicity) of its decay product. Example : $\tau^- \to \pi^- \nu_\tau$.

At the τ^- rest frame

$$\cos\theta_\pi = \hat{n}_\tau . \hat{p}_\pi, \quad \frac{1}{\Gamma_\pi}\frac{d\Gamma_\pi}{d\cos\theta_\pi} = \frac{1}{2}(1 + \kappa_\pi P \cos\theta_\pi)$$

The distribution can be written in term of energy fraction $x_\pi = E_\pi / E_\tau$ so that

$$\frac{1}{\Gamma_\pi}\frac{d\Gamma_i}{dx_\pi} = 1 + \kappa_\pi P(2x_\pi - 1),$$

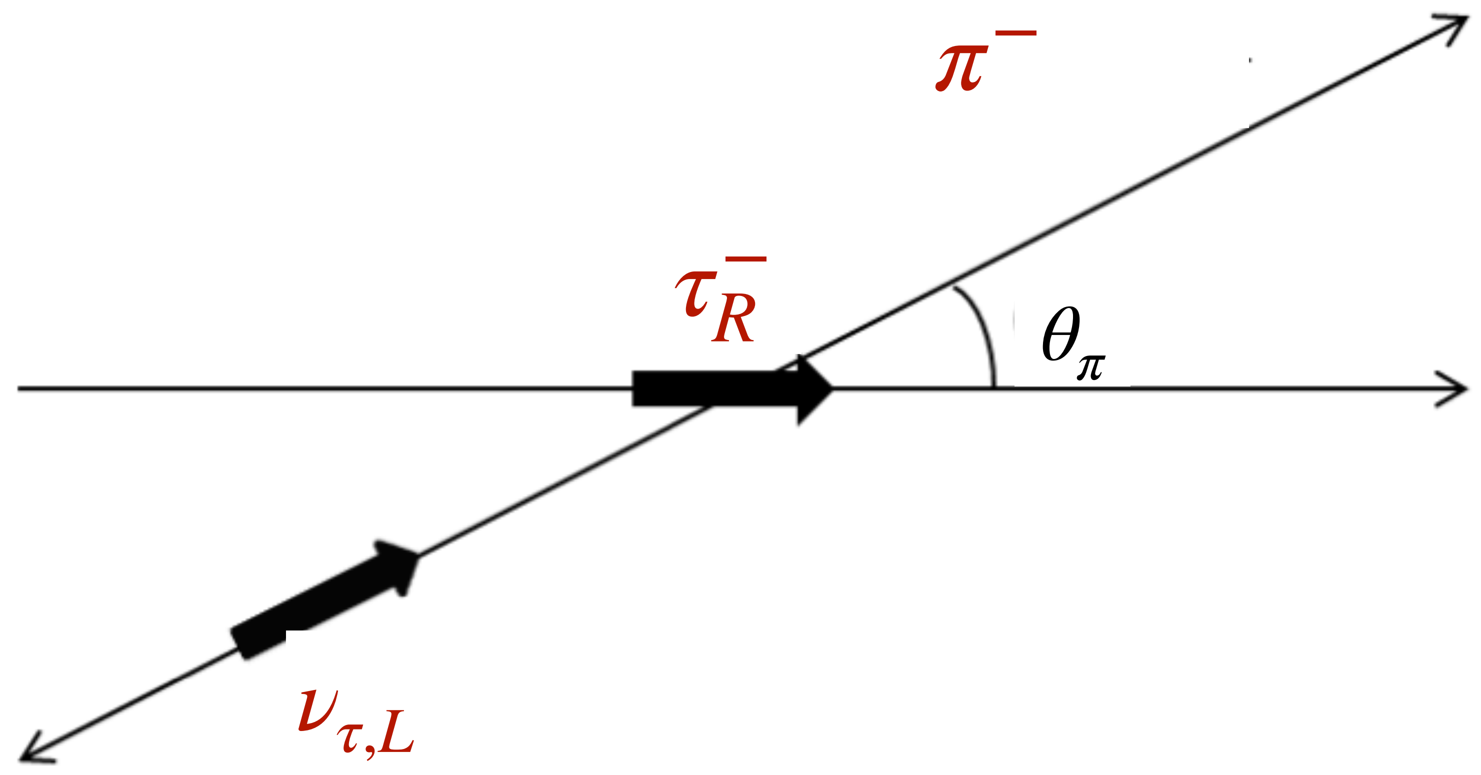

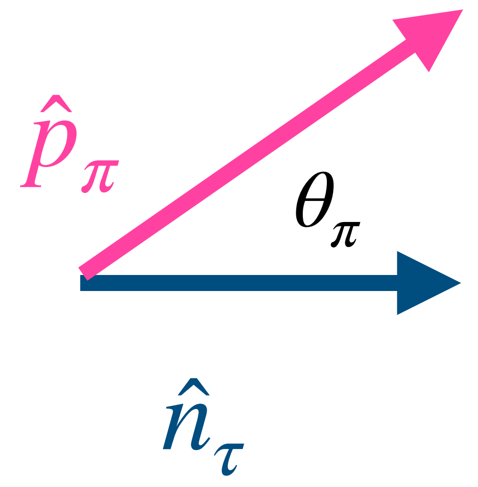

$\kappa_i \in [-1,1]$ is spin analyzing power.

P=± 1 is positive or negative helicity.

$$\cos\theta = \frac{2x_\pi - 1 - a^2}{\beta(1 - a^2)}$$

$a = m_\pi / m_\tau, a \approx 0$ for π

$\beta = \sqrt{1 - m_\tau^2 / E_\tau^2} \approx 1$ (in collinear limit)

Tau decay products distribution

$$x_i = E_i/E_\tau$$

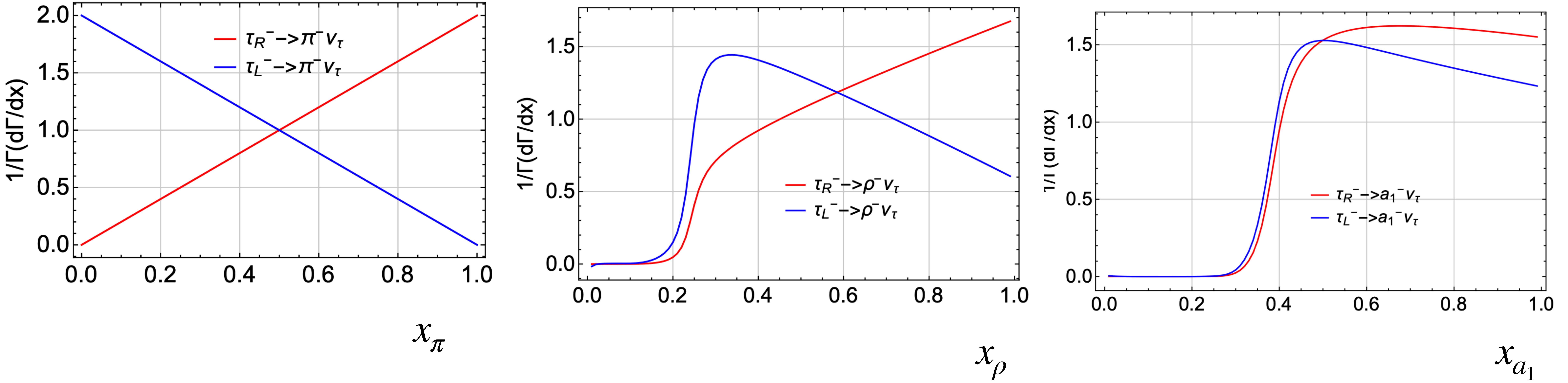

- The dominant hadronic tau (τ_h) decay products : π, ρ, a_1 (up to 50% of tau BR).
- Clear separation between τ_R, τ_L : τ_R dominate high x_i , and τ_L is vice versa.
- Modification on the x_i distributions of ρ, a_1 come from their κ_i. (All labels should be able to be read)

[Bullock, et. al., Nucl. Phys. B, 395:499, (1993)].

Chirality structure (problem*)

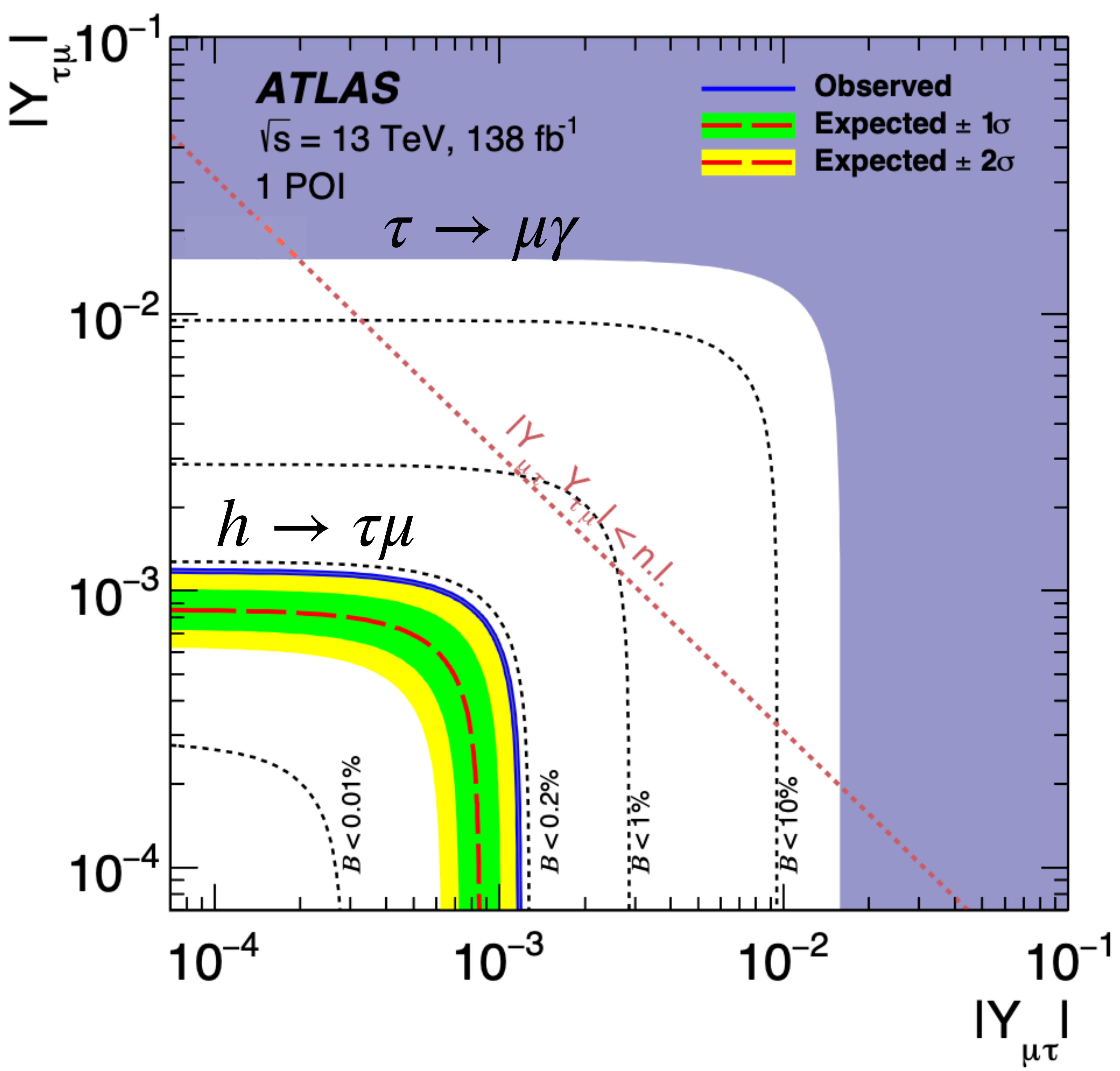

ATLAS, JHEP 07, 166 (2023)

$$\bar{y}_{\tau\mu} = \sqrt{|y_{\tau\mu}|^2 + |y_{\mu\tau}|^2} < 1.2 \times 10^{-3}$$

- Experimental: effect of chirality structure on hLFV has not been observed.

  At the upper limit contour :

  $BR(h \to \tau\mu) \sim |y_{\tau\mu}|^2 + |y_{\mu\tau}|^2 <$ some number.

  $\to (y_{\mu\tau}, y_{\tau\mu})$

- No spin correlation effects:

  $BR(h \to \tau_L \mu_R) \sim |y_{\tau\mu}|^2$, -> (0,b)

  $BR(h \to \tau_R \mu_L) \sim |y_{\mu\tau}|^2$, -> (a,0)

- Unpolarized (no chiral structure) : a=b or $\bar{y}_{\tau\mu}$ is a constant . Circle in $y_{\mu\tau} - y_{\tau\mu}$ plane.
- Polarized case, a≠b and $\bar{y}_{\tau\mu}$ is not a constant.

Theoretically : models with a chiral hLFV has interesting phenomenology.

Example in [C. W. Chiang, et. al., JHEP 11 (2015) 057] : 2HDM + singlet scalar σ.

$U(1)_{\rm PQ}$ charge : (0, -1, +1) for Φ_1, Φ_2, σ.

σ gets a vev at high energy scale, so in low energy, the theory is 2HDM.

τ_R also has a -1 PQ charge.

$$\mathscr{L}_Y \supset \bar{l}_{Li}(Y_1)_{ia}\Phi_1 l_{Ra} + \bar{l}_{Li}(Y_2)_{i3}\tau_R + h.c., \quad i = 1,2,3, \quad a = 1,2$$

Rotate to the eigen mass basis, both for the Higgs doublets and the leptons :

$$\mathscr{L}_Y \supset -\sum_l \xi_l \frac{m_f}{v}\bar{l}l - a \sum_{l,l'=e,\mu,\tau} (H_l)_{ll'}\frac{m_l}{v}h\bar{l}_L l'_R + h.c.$$

$$H_e = V_L \begin{pmatrix} 0 & & \\ & 0 & \\ & & 1 \end{pmatrix} V_L^\dagger - \begin{pmatrix} 0 & & \\ & 0 & \\ & & 1 \end{pmatrix}, \quad a = (\tan\beta - cot\beta)\cos(\beta - \alpha),$$

$$\xi_l = \begin{cases} \sin(\beta-\alpha) + \cot\beta\cos(\beta-\alpha), \text{ for } (\mathrm{l} = \tau) \\ \sin(\beta-\alpha) - \tan\beta\cos(\beta-\alpha) \text{ for } (\mathrm{l} \neq \tau) \end{cases}$$

Result: In $h \to \tau^-\mu^+$, the τ is left handed for some benchmark parameters.

- The ATLAS number is recovered for m_{col2} for $x_{1,2} > 0$ with difference in S and B average to 30% and 7% respectively.

Cuts

- Baseline cuts.

1. Exactly 1 isolated μ and 1τ jet (opposite sign) with $p_{T,\mu} = 27.3\ \mathrm{GeV}$ and $p_{T,\tau_{\rm vis}} = 25\ \mathrm{GeV}$. $\tau_{\rm vis}$ denotes the visible decay product of tau jet, i.e. π, ρ or a_1
2. To reduce background from misidentified τ, we need $|\Delta\eta(\mu, \tau_{\rm vis})| < 2.0$.
3. To avoid $\not{E}_T$ coming from other source, we need $\sum_{i=\mu,\tau_{\rm vis}} \cos\Delta\phi(i, \not{E}_T) > -0.35$.

- Further signal-background separation is done by using collinear mass $m_{\rm col}$ analysis : two missing particles and one missing particle.

Collinear mass m_{col2}

- Commonly used for reconstructing $m_{\tau\tau}$ of $h \to \tau\tau$. We call this m_{col2}.
- At high energy/high-p_T condition, the decay products of tau (visible or not) will be collinear to the tau momentum.

  $\vec{p}_{\tau_{\text{vis}}} = x\vec{p}_\tau, \quad \vec{p}_{\tau_{\text{invis}}} = (1-x)\vec{p}_\tau, \quad 0 \le x \le 1.$
- The $\vec{\not{p}}_T$ accounts for the two neutrinos from the $h \to \tau\tau$:

  $\vec{\not{p}}_T = c_1\vec{p}_{T,\tau_{1\text{vis}}} + c_2\vec{p}_{T,\tau_{2\text{vis}}}, \quad c_i = (1-x_i)/x_i > 0.$
- Solving for c_1, c_2, we can reconstruct the $m_{\tau\tau}$ mass as

  $m^2_{\text{col2}} = (p_{\tau_{1\text{vis}}} + p_{\tau_{2\text{vis}}} + p_{\nu_{1\text{reco}}} + p_{\nu_{2\text{reco}}})^2$, where $\vec{p}_{\nu_{i\text{reco}}} = c_i\vec{p}_{\tau_{i\text{vis}}}$.
- For the $m_{\tau\mu}$, we assume the μ to be the visible product of τ_2, i.e. $\tau_{2,\text{vis}}$. [short sentences only]

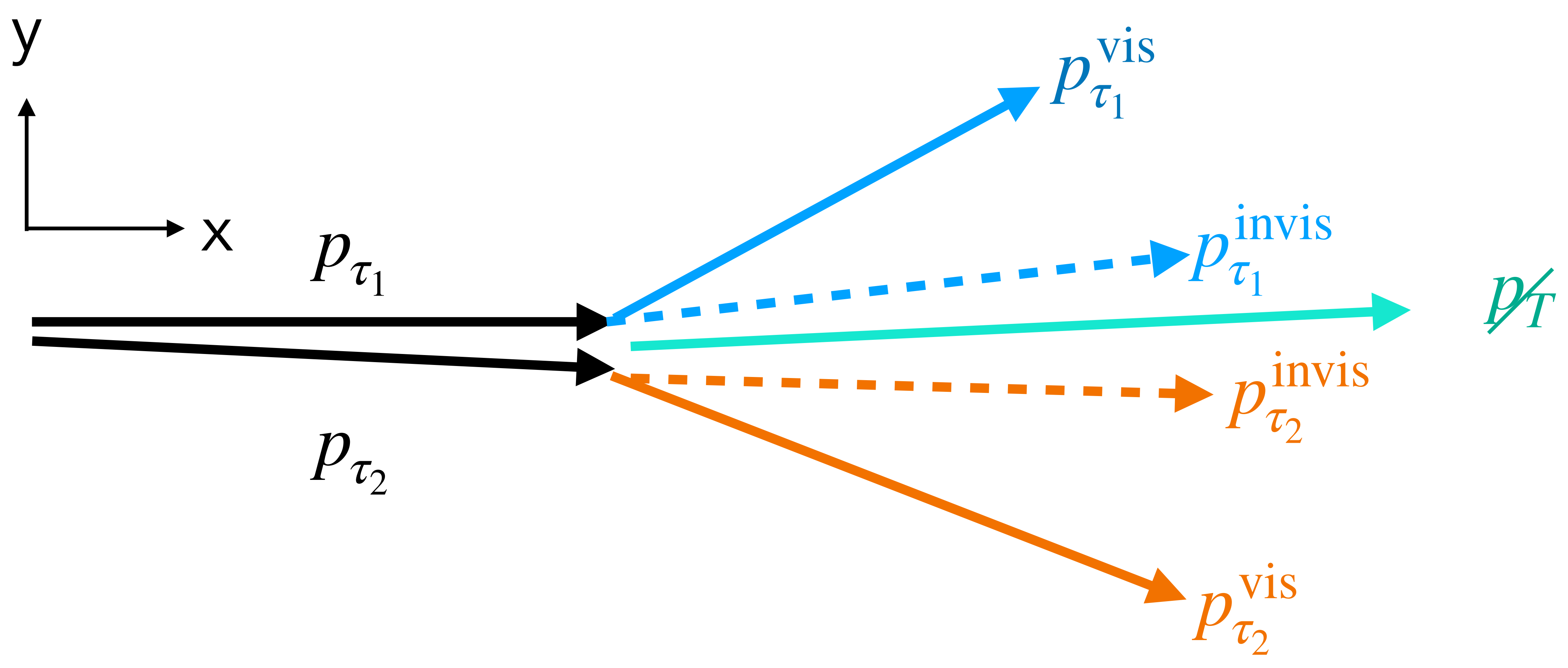

Collinear mass m_{coll}

- A better natural way of reconstructing the $m_{\tau\mu}$ is by assuming one missing particle.
  $\vec{\not{p}}_T \propto c_1 \vec{p}_{T,\tau_{1\text{vis}}}$.
- However due to the detector and measurement effects, the $\vec{\not{p}}_T$ is not completely parallel with $\vec{p}_{T,\tau_{1\text{vis}}}$.
  $\vec{\not{p}}_T = c_1 \vec{p}_{T,\tau_{1\text{vis}}} + c_\perp \hat{n}_{T,\perp}$, where $\hat{n}_{T,\perp}$ is the unit vector orthogonal to $\vec{p}_{T,\tau_{1\text{vis}}}$.
- Solving for c_1 from $\cos\theta = \vec{\not{p}}_T \cdot \vec{p}_{T,\tau_{1\text{vis}}} / |\vec{\not{p}}_T||\vec{p}_{T,\tau_{1\text{vis}}}|$, we can reconstruct the $m_{\tau\mu}$ mass as
  $m^2_{\text{coll1}} = (p_{\tau_{1\text{vis}}} + p_{\nu_{1\text{reco}}} + p_\mu)^2$, where $\vec{p}_{\nu_{1\text{reco}}} = c_1 \vec{p}_{\tau_{1\text{vis}}}$.

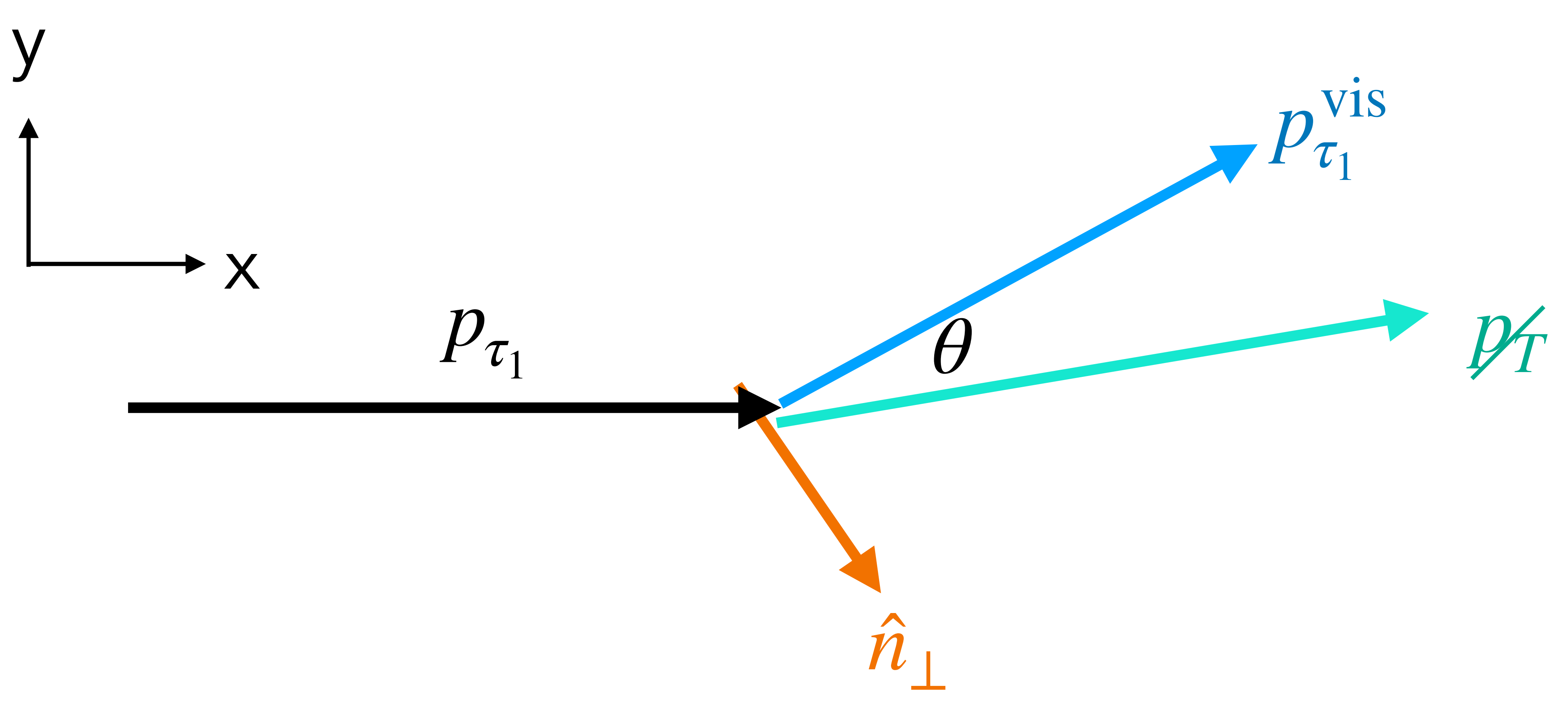

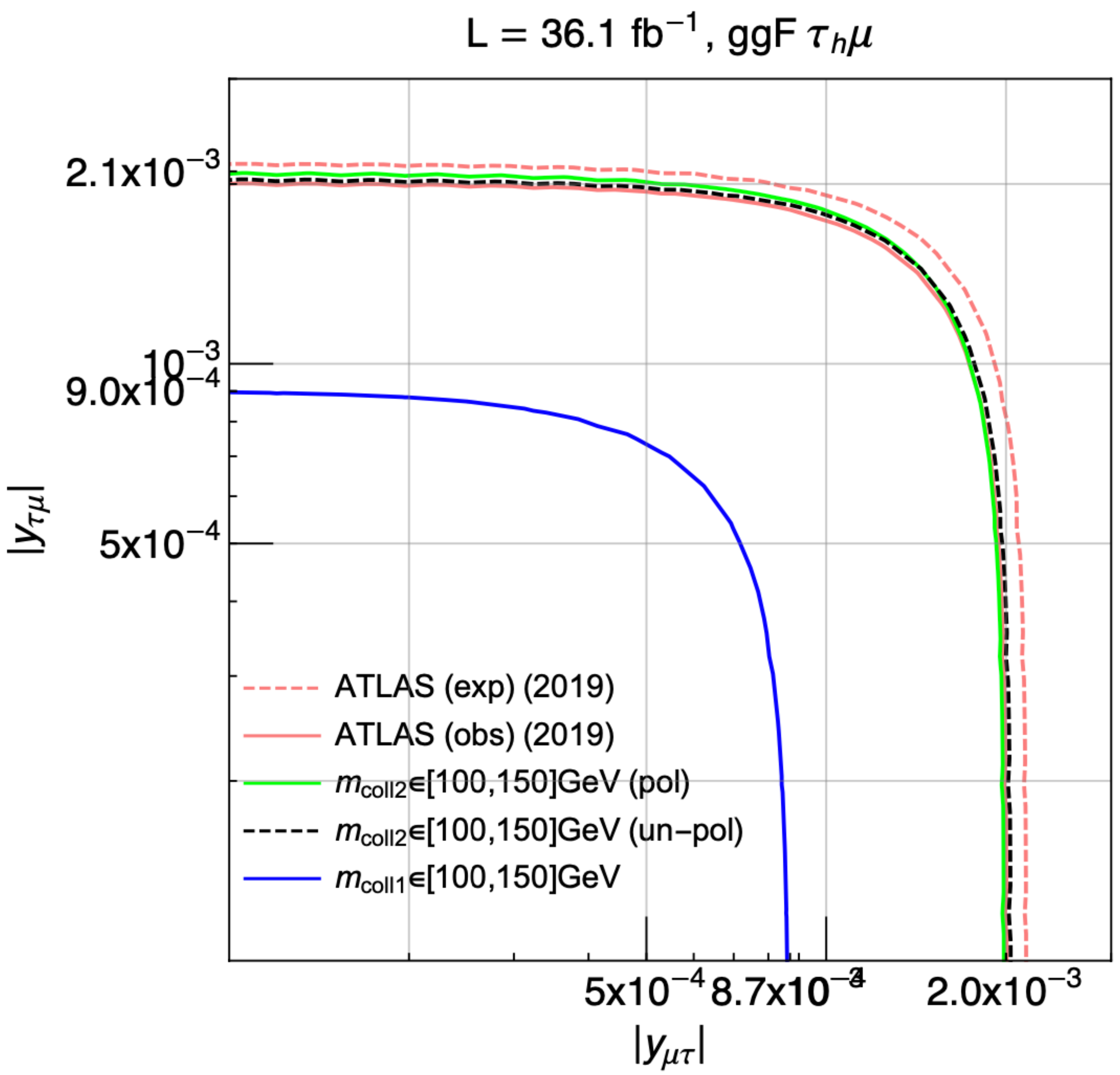

From 95%CL BR we can get $\bar{y}_{\tau\mu,L}, \bar{y}_{\tau\mu,R}$ at 95% CL using:

$$\mathrm{BR}^{95\%}_{R,L} = 0.12\% \times \frac{\bar{y}^2_{\tau\mu\ R,L}}{10^{-6}}$$

$$f(x) = af(x)_R + (1-a)f(x)_L$$

- For $\Delta m = 25$ GeV, the sensitivity is improved 5 times from $m_{\rm col2}$ to $m_{\rm col1}$.
- Coincidentally $m_{\rm col2}$ sensitivity is close to the non-VBF $\tau_h\mu$ mode ATLAS with $\mathrm{BR}(h \to \tau\mu) = 0.57\,\%$ or $\bar{y}_{\tau\mu} = 0.0022$ (pink dashed line). [1]
- If we include the systematic errors, our result may be invalid, however the $m_{\rm col1}$ has a better sensitivity should persist. [this is the last one]
- The chirality effect on the sensitivity $\bar{y}_{\tau\mu}$ modifies the contour from circle into ellipse.
- It modifies $\pm 4-6\,\%$ on BR or $\pm 2-3\,\%$ on the unpolarized $(y_{\mu\tau}, y_{\tau\mu})$ plane. We expect similar modification on the ATLAS result also.

LFV experiments status

The LFV interaction $h \to l_i l_j$ leads to important (low-energy) LFV processes that has been experimentally on.

Process	BR present bound	Future sensitivity
$\mu \to e\gamma$	3.1×10^{-13}[1]	6×10^{-14}[2]
$\tau \to e\gamma$	3.3×10^{-8} [3]	$\sim 10^{-9}$ [4]
$\tau \to \mu\gamma$	4.4×10^{-8} [3]	$\sim 10^{-9}$[4, 5]
$\mu \to eee$	1.0×10^{-12}[6]	$\sim 10^{-16}$ [7]
$\tau \to eee$	2.7×10^{-8}[8]	$\sim 4 \times 10^{-10}$[5]
$\tau \to \mu\mu\mu$	2.1×10^{-8}[8]	$\sim 5 \times 10^{-10}$ [5]
$\tau^- \to e^-\mu^+\mu^-$	2.7×10^{-8}[8]	$\sim 5 \times 10^{-10}$ [5]
$\tau^- \to \mu^-e^+e^-$	1.8×10^{-8}[8]	$\sim 5 \times 10^{-10}$ [5]
$\tau^- \to e^+\mu^-\mu^+$	1.7×10^{-8}[8]	$\sim 4 \times 10^{-10}$ [5]
$\tau^- \to \mu^+e^-e^+$	1.5×10^{-8}[8]	$\sim 3 \times 10^{-10}$ [5]

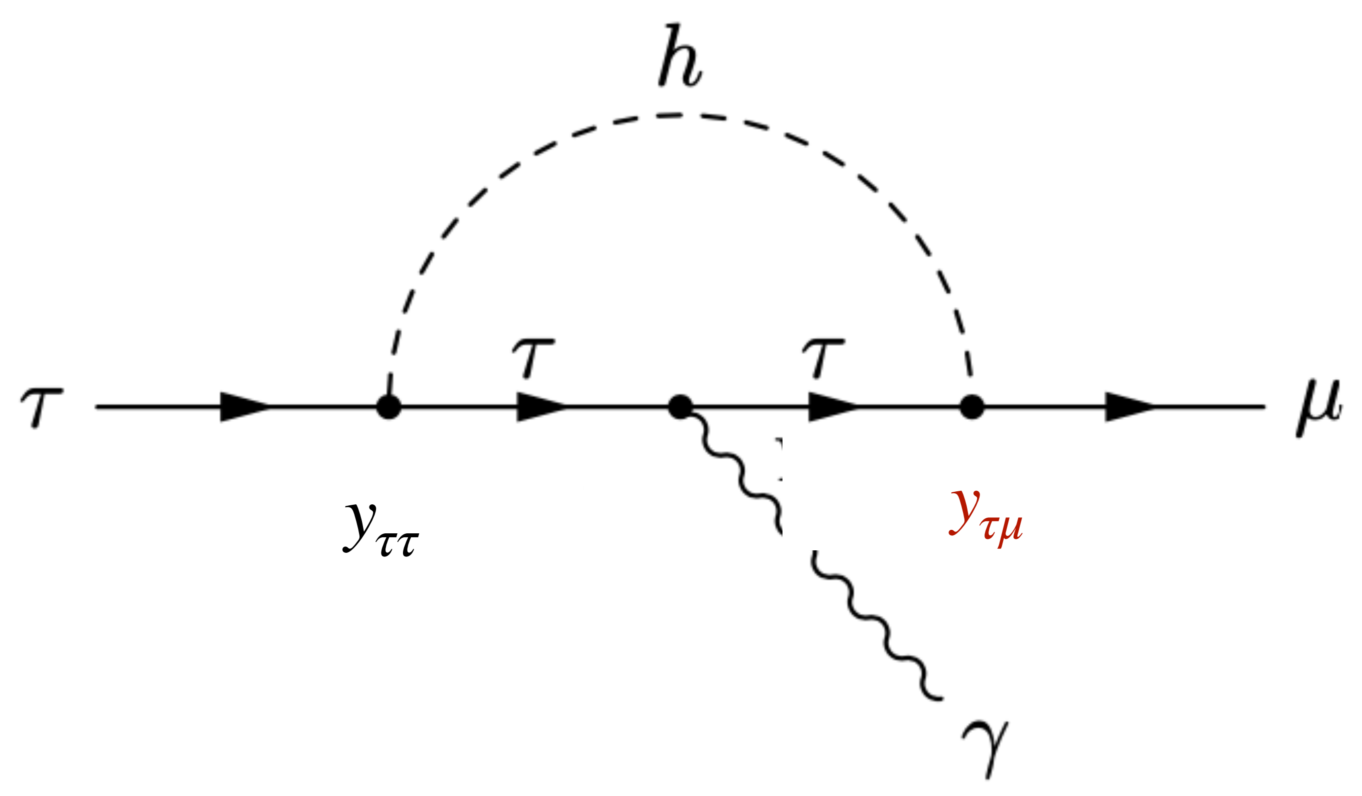

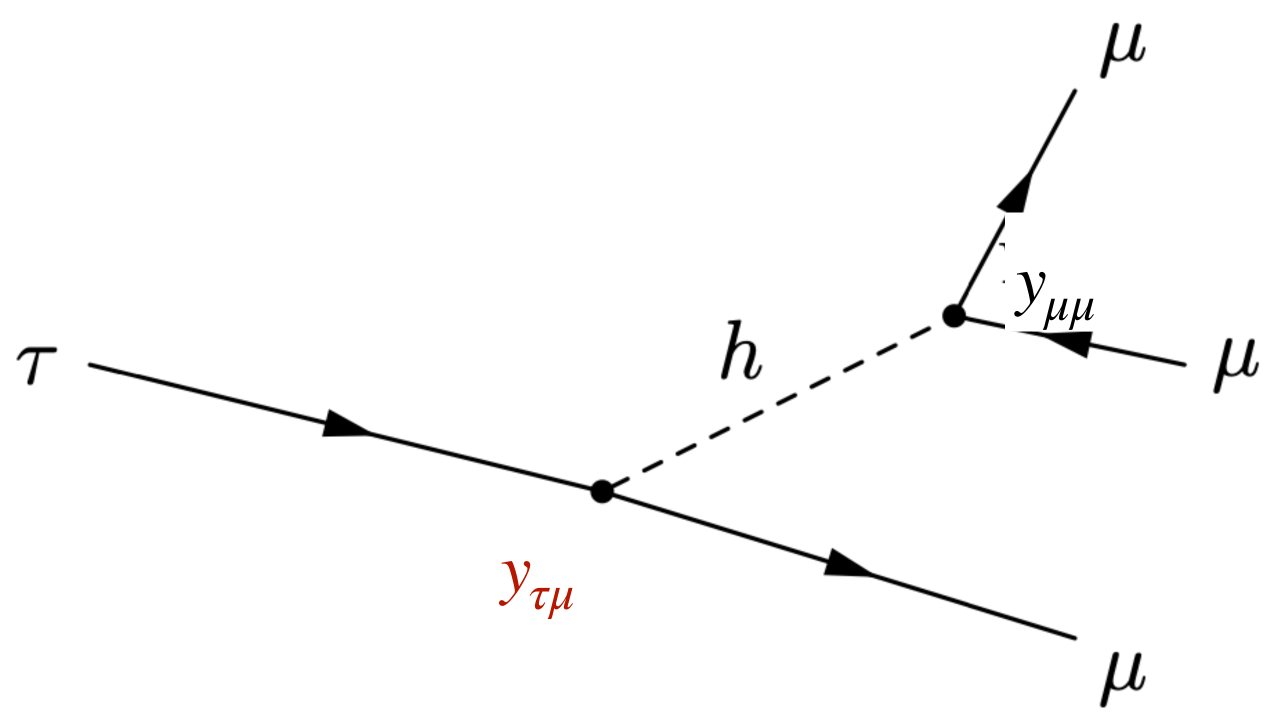

[1] MEG-II, arXiv: 2310.12614
[2] A. M. Baldini, et.al. (MEG proposal), arXiv:1301.7225
[3] BaBar, Phys. Rev. Lett. 104, 021802 (2010)
[4] BaBar, Belle, Eur. Phys. J. C 74, 3026 (2014)
[5] Belle-II, PTEP 2019, 123C01 (2019), Err: PTEP 2020, 029201 (2020)
[6] SINDRUM, Nucl. Phys. B 299, 1 (1988)
[7] A. Blondel et al. (Mu3e proposal), arXiv:1301.6113
[8] Belle, Phys. Lett. B 687, 139 (2010)

Cut flows for collinear mass analysis L=36.1 fb^{-1}

Signal (S) Background (B)

		$h \to \tau\mu_{(BR=1\ \%)}$ τ_R	τ_L	$Z \to \tau_h \tau_\mu$	$S^{95\%}$	$\text{BR}^{95\%}$ τ_R	τ_L
	σ at 13 TeV LHC	355 fb		258 pb			
	for $\mathcal{L} = 36.1\text{fb}^{-1}$	12795		9.31×10^6			
	baseline cuts	1979	1742	130147			
$x_i = 1/(c_i + 1)$	$x_1 > 0$ and $x_2 > 0$	1672	1480	102536	747	0.45	0.50
m_{coll2}	$\|m_{\text{coll2}} - m_h\| < 25$ GeV	717	643	21473	342	0.48	0.53
	$\|m_{\text{coll2}} - m_h\| < 10$ GeV	344	304	7639	204	0.59	0.67
	$\|m_{\text{coll2}} - m_h\| < 5$ GeV	177	157	3776	143	0.81	0.91
	$c_1 > 0$	1765	1608	68602	610	0.34	0.38
m_{coll1}	$\|m_{\text{coll1}} - m_h\| < 25$ GeV	1626	1493	4023	148	0.091	0.099
	$\|m_{\text{coll1}} - m_h\| < 10$ GeV	1080	1008	639	58.9	0.055	0.059
	$\|m_{\text{coll1}} - m_h\| < 5$ GeV	617	577	216	34.2	0.056	0.059

Notes:

1. The number of events are normalized to ATLAS 36.1 fb^{-1}.
   [Phys. Lett. B 800, 135069 (2020)]
2. $S^{95\%} = 1.65\sqrt{B}$ is the one-sided 95% CL upper bound on the signals.
3. $BR^{95\%} = (S^{95\%}/S)\text{BR}(h \to \tau\mu)$, with $\text{BR}(\text{h} \to \tau\mu) = 1\,\%$.

S/B

- $\Delta m = 25$ GeV, m_{col2} (blue -> pink) reduces B and S: 0.23% and 5-6%. m_{col1}(blue -> orange) reduces B and S: 0.04% and 12-13%. S/B in m_{col1} is better than m_{col2}.
- S/B increases for smaller Δm. m_{col1} S/B is 2.8 for $\Delta m = 5$GeV (magenta). Better S/B is needed because no systemic errors considered. m_{col1}, $\Delta m = 5$ GeV (best analysis)

Chirality structure

- Asymmetric behavior exists in all cut flow with τ_R survives more efficiently than τ_L.
- Δm=25→5 GeV, S deviation from unpolarized(*) case is $\pm 6\,\%$ for m_{col2} and $\pm 4.5 \to 3.3\,\%$ for m_{col1}.

(*) unpolarized = average between R and L.